JACS
JOURNAL OF THE AMERICAN CHEMICAL SOCIETY
Perspective
pubs.acs.org/JACS

Recent Achievements on Inorganic Electrode Materials for Lithium-Ion Batteries

Laurence Croguennec[†,‡,#] and M. Rosa Palacin*[,§,‡]

[§]Institut de Ciència de Materials de Barcelona, ICMAB-CSIC, Campus de la UAB, 08193 Bellaterra, Catalonia, Spain
[†]CNRS, University of Bordeaux, ICMCB, UPR 9048, 33600 Pessac, France
[‡]ALISTORE-ERI European Research Institute
[#]RS2E, Réseau Français sur le Stockage Electrochimique de l'Energie, CNRS FR3459, 80039 Amiens Cedex, France

ABSTRACT: The lithium-ion battery technology is rooted in the studies of intercalation of guest ions into inorganic host materials developed ca. 40 years ago. It further turned into a commercial product, which will soon blow its 25th candle. Intense research efforts during this time have resulted in the development of a large spectrum of electrode materials together with deep understanding of the underlying structure−property relationships that govern their performance. This has enabled an ever increasing electrochemical yield together with the diversification of the technology into several subfamilies, tailoring materials to application requirements. The present paper aims at providing a global and critical perspective on inorganic electrode materials for lithium-ion batteries categorized by their reaction mechanism and structural dimensionality. Specific emphasis is put on recent research in the field, which beyond the chemistry and microstructure of the materials themselves also involves considering interfacial chemistry concepts alongside progress in characterization techniques. Finally a short personal perspective is provided on some plausible development of the field.

1. INTRODUCTION

Lithium-ion batteries entered the market in the 1990's and are currently a very well established and familiar commercial product. Its development parallel to the boost of the consumer electronic market is a striking example of synergistic application driven product development with continuous research resulting in incremental performance improvement. In addition to that, recent concerns to decrease societal dependence on fossil fuels through electrification of transportation are opening a new market for this technology, involving larger scale storage and hence a somewhat different set of requirements. Last but not least, the imperious need to implement electrical energy storage in the grid to ensure reliability of supply while enhancing renewable penetration has brought about a re-evaluation of the energy storage technologies available to these even larger scale applications. In spite of some concerns related to cost and risk lithium supply, the potential of lithium-ion technology for such a purpose has been identified, and several demonstration projects are currently on going worldwide.

The above-discussed strategic trends have prompted massive and intense research efforts to improve batteries in terms of energy and power density, safety, cycle life, cost, environmental aspects, etc. Indeed, requirements for transport applications are specially challenging as enhanced safety is mandatory and energy density determines the vehicle autonomy range. Such efforts (e.g., almost 6000 records published in 2013 related to lithium-ion technology) emerge both from the industrial and academic research communities, the strong interaction between them deserving special mention.

In a historical perspective, the study of intercalation reactions by the inorganic solid-state chemistry community[1] turned out to be a cornerstone in the battery development. Indeed, the potential of suitable host compounds to allow reversible (usually topotactic) insertion and deinsertion of lithium ions, without major structural changes while exhibiting suitable redox chemistry thanks to the presence of transition metals, was soon realized. The initial prospects of building extremely high energy density secondary cells using lithium metal anodes and conventional organic solvent-based electrolytes had to be soon dismissed due to issues related to non-uniform lithium plating (unsurprising when considering classical electroplating notions) which resulted in unacceptable safety risks. Lithium-based alloys appeared as the first natural solution to replace lithium metal, but proved unsuccessful due to the large volume changes involved in the electrochemical alloying−dealloying processes, which ultimately resulted in severe capacity fading upon cycling. The bottleneck for commercialization was overcome by returning to square one concepts by selecting a negative electrode (low potential) material also operating through an intercalation redox mechanism. Following this approach, the use of substantially different materials to those proposed for the positive electrode (high potential) was compulsory to enable cell operation potentials outperforming those of aqueous electrolyte nickel and lead-based cells which were state-of-the art technologies at the time. Thus, early lithium-ion batteries consisted of $LiCoO_2$ and graphite at the positive and negative electrode, respectively. After 25 years of development, the concept remains the same, but the spectrum of materials used in commercial cells has widened to the extent that several large families of lithium-ion technologies exist.

In practical lithium-ion batteries the electrodes are conventionally tape casted on a metal current collector (aluminum for the positive and copper for the negative) and aside the active materials contain additives to enhance electronic conductivity

Received: July 31, 2014
Published: February 13, 2015

DOI: 10.1021/ja507828x
J. Am. Chem. Soc. 2015, 137, 3140−3156

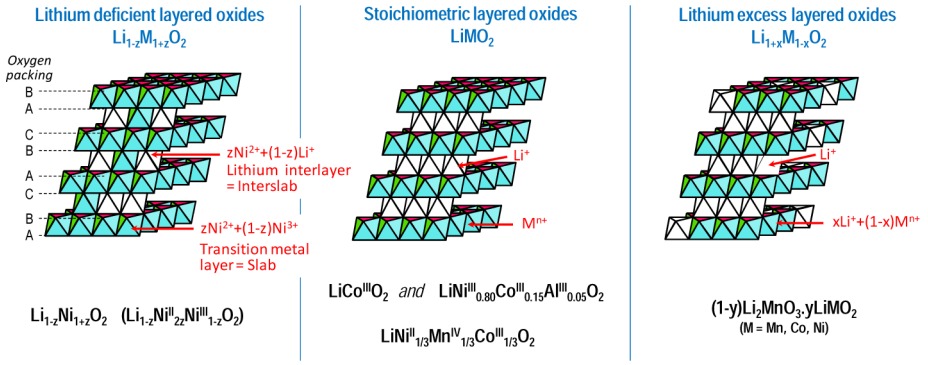

Figure 1. Scheme depicting the crystal structure of layered Li-M-O oxides with different compositions and cation distributions.

(typically carbon black) and a binder (e.g., polyvinylidene fluoride, PVDF) to improve adhesion, mechanical strength, and ease of processing. Positive and negative electrodes are separated by a microporous film (such as polyethylene or polypropylene), and the whole assembly is impregnated with the electrolyte. The electrolyte solvents commonly used (mixtures of different alkyl carbonates) are in fact unstable below ca. 0.8 V vs Li^+/Li and above ca. 4.5 V vs Li^+/Li in the presence of electrode materials, which depending on their state of charge/discharge can be strongly oxidizing/reducing.[2] Degradation reactions do often involve the electrolyte salt (usually $LiPF_6$) and water traces, which can result in formation of HF and lead to transition metal dissolution. The resulting insoluble products, however, form a solid passivation layer (the solid electrolyte interphase, SEI) at the surface of the negative electrode.[3−5] An interphase is also formed at the surface of the positive electrode, sometimes denoted the surface layer (SL). Thus, the use of present electrolytes during cell operation is entirely made possible through proper chemical passivation of electrode surfaces.

Since the operation principle of the lithium-ion technology together with its evolution were already discussed in a recent perspective paper in this journal,[6] the present paper focuses on key recent advances and identification of existing bottlenecks in the field. As the global aim is to inspire future research to overcome existing challenges which will certainly benefit from a diversity of perspectives coming from different backgrounds and scientific domains, special effort has been taken to direct the text to the non-specialized readership hoping that this will serve as a springboard for further reading.

2. INSERTION ELECTRODES

As mentioned above, current commercial lithium-ion batteries use electrode materials exhibiting an insertion redox reaction mechanism for both the positive and negative electrodes, which results in electrochemical capacities limited to one electron per transition metal. Such materials can be classified according to the dimensionality of their structural framework (3D or 2D). Nonetheless, it has to be highlighted that this is not necessarily related to the diffusion pathways of lithium ions in the structure. For instance, $LiMn_2O_4$ and $LiFePO_4$ are both hosts exhibiting a 3D structure with the lithium diffusion being 3D in the former but only 1D in the latter.[7] Most of the materials developed exhibit high insertion potentials and are thus suitable for use as positive electrode materials. The spectrum of insertion negative electrode materials is much more limited owing to (i) the very good performance of graphitic materials, which prompted only limited research efforts as compared to those devoted to the positive counterparts, and (ii) the need of low operation potentials, which limits the choice of redox centers available.

The next sections are devoted to the discussion of recent research achievements in the field of insertion electrode materials, both 2D (graphite and layered oxides) and 3D (spinel and polyanionic).

2.1. 2D Structures. Most types of carbon react with lithium ions at low potential (~0.1−1 V vs Li^+/Li) and are thus suitable for use as negative electrode materials. The amount of lithium reversibly incorporated in the carbon lattice (the reversible capacity), the faradaic losses during the first cycle (the irreversible capacity), and the profile of the potential composition profile can exhibit important differences.[8] Indeed, the redox process is strongly influenced by macro- and microstructural features including the specific surface, surface chemistry,[9] morphology, crystallinity, and orientation of the crystallites.[10] Hard carbons can deliver high capacity since the random alignment of small-dimensional graphene layers provides significant porosity able to accommodate lithium,[11] yet with an irreversible capacity higher than that of graphite. Their rate capability (power performance) is also usually limited as their volumetric capacity is penalized by a lower density. The generalized use of graphite electrodes in commercial batteries was enabled by the development of ethylene carbonate (EC)-based electrolytes, which form an effective SEI that prevents exfoliation[12] due to solvent co-intercalation. Its full reduction involves the formation of LiC_6 (with 372 mAh/g and 975 mAh/cm^3 gravimetric and volumetric capacity, respectively).

On the positive side, the layered oxide $LiCoO_2$ (Figure 1) remains widely used as positive electrode in lithium-ion batteries for portable devices, as it delivers attractive volumetric energy density, excellent cyclability, and high rate capability. The main caveat of this compound is its low reversible capacity; equivalent to the exchange of a mere 0.5 Li+ ions per mol of Co and thereby limited to ca. 150 mAh/g, even if surface modifications have allowed increasing the upper voltage limit of operation and thus the reversible capacity, with the exchange of up to 0.7 Li^+ per Co.[13] The microstructure of the material itself is also in constant evolution in order to increase the tap density and the volumetric energy density. Nevertheless, its use in large-format batteries is prevented by its high cost and limited thermal stability of the oxidized $Li_{1-x}CoO_2$ phase which may create safety concerns. This feature is common to all layered $Li_{1-x}MO_2$ for $x < 1/2$ with oxygen being released from the lattice and reacting with the electrolyte solvents through exothermic reactions. Reduction of the transition metal ions

DOI: 10.1021/ja507828x
J. Am. Chem. Soc. 2015, 137, 3140−3156

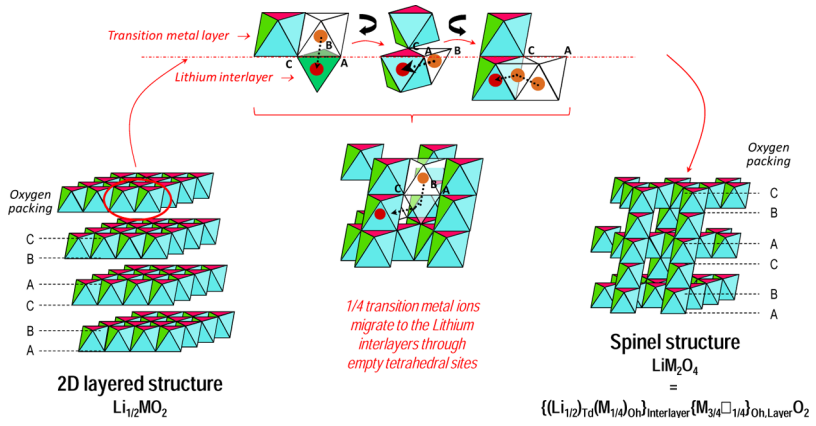

Figure 2. Scheme depicting the pathway for layered to spinel structural transition observed for deintercalated layered oxides Li_xMO_2 at high temperature (Td and Oh, for tetrahedral and octahedral sites, respectively). Note that for the sake of simplicity lithium ions are not represented. Adapted with permission from:[14] Guilmard, M.; Croguennec, L.; Denux, D.; Delmas, C. *Chem. Mater.* **2003**, *15*, 4476. Copyright (2003) American Chemical Society.

occurs together with migration of ca. 25% of the transition-metal ions from the metal layer to the lithium interlayer through empty tetrahedral sites (Figure 2) causing a structural transformation from layered 2D to spinel 3D with the oxygen lattice remaining unaffected (AB CA BC packing with A, B, and C being the three positions of a triangular lattice).

$LiNi^{III}O_2$, isostructural to $LiCoO_2$, was early considered as a possible lower cost alternative, but its synthesis as a pure stoichiometric 2D compound is difficult to achieve. Indeed, $Li_{1-z}Ni_{1+z}O_2$ ($z > 0$) is most commonly obtained, with the presence of extra nickel ions in the interlayer lithium sites (Figure 1) and is thus, as such, of limited interest. Partial cobalt and aluminum substitutions for nickel were shown to be the key to control the 2D character of the structure,[15] bringing also enhanced thermal stability, the optimum composition being $LiNi^{III}_{0.80}Co^{III}_{0.15}Al^{III}_{0.05}O_2$ (NCA, reversible capacity of 185 mAh/g involving mainly the Ni^{3+}/Ni^{4+} redox couple at an average voltage of 3.7 V vs Li^+/Li (Figure 1)). $LiNi^{II}_{1/3}Mn^{IV}_{1/3}Co^{III}_{1/3}O_2$ (NMC) exhibits an even higher thermal stability in the delithiated state, due to the stabilization effect of the tetravalent manganese ions,[16,17] and even if the manganese ions do not participate in the redox processes, this compound exhibits an attractive reversible capacity of 170 mAh/g at an average voltage of 3.7 V vs Li^+/Li. Such improvements paved the way for the commercial use of NCA and NMC in larger cells for transport applications, even if they remain expensive due to the cost of both nickel and cobalt. NCA is more attractive for high rate applications due to its higher electronic and ionic conductivities (electron hopping among nickel ions promotes faster lithium diffusion within the structure), as ordering of the Ni, Mn, and Co ions in NMC is detrimental to electron mobility (Figure 1).

An attractive strategy which, in our opinion, deserves to be widely explored has been reported in the past few years by Y. K. Sun et al. to further optimize the energy density and thermal stability of Ni-rich layered oxides by developing core−shell or full gradient composition materials.[18,19] For instance, $Li-Ni_{0.80}Co_{0.10}Mn_{0.10}O_2$ at the core provides high capacity, while $LiNi^{II}_{1/2}Mn^{IV}_{1/2}O_2$ at the surface ensures high thermal stability. While difficulties may be encountered to prepare an homogeneous material at large scale, fine control of the process parameters (pH, pumping rates of the precursors, stirring conditions, etc.) is certainly the path to success.

The family of layered materials currently attracting most interest is that of Li- and Mn-rich layered oxides (commonly denoted $(1-y)Li_2MnO_3{\cdot}yLiMO_2$ (M = Mn, Co, Ni), with the overall Li/M ratio >1) (Figure 1) which exhibit very high energy densities at an affordable cost.[20−22] They have been described alternatively either as composites[20,23−25] or "solid solutions"[26−31] between $Li_2Mn^{IV}O_3$ and layered $LiM^{III}O_2$ with, in both cases, a certain degree of cation (Li, M, Mn) ordering within the transition metal layers. The control of the composition and structural features of these materials is tricky as revealed by all the apparent discrepancies reported, with the oxygen partial pressure and the thermal history (intermediate treatment at low temperature, heating and cooling rates, etc.) being critical synthesis parameters to prevent phase separation,[32−36] while a rigorous control of the stoichiometry (a ratio close to 1:2 between the larger and the smaller cations) and oxidation state of each transition metal are crucial to achieve extended cation ordering.[37] The control of the composition and local structure enables tuning the formation of a 3D percolating vacancy pathway for fast lithium diffusion in these 2D structures and yielding thereby optimized electrochemical capacity and rate capability: $x = 1.09$ is found to be the percolation threshold for $Li_xM_{2-x}O_2$ (whatever their structure: layered, spinel, disordered, or rock-salt), while $x > 1.22$ allows reaching a reversible capacity of 1 Li^+ per transition metal.[38]

A common feature for all Li-rich layered oxides is a long (i.e., high capacity) "plateau", observed only at the end of the first oxidation (Figure 3), once all the transition metal ions have already reached the tetravalent state. Lu et al. proposed that the charge compensation mechanism for lithium-ion deintercalation was oxygen loss,[39] but even if confirmed by *in situ* differential electrochemical mass spectrometry (DEMS),[40] its amount was shown to be too low to counterbalance all the lithium ions deintercalated during the "plateau". The observed behavior can only be explained through the reversible participation of oxygen anions in the redox processes thanks to hybridization between their p and the d levels of the transition metal,[41−43] which increases with enhancing electronegativity and oxidation state (Figure 4). This reaction is reversible within the bulk, occurring without any major structural modification, while at the surface, oxidized oxygen ions are destabilized and lost causing structural reorganization and transition metal migration with concomitant formation of

DOI: 10.1021/ja507828x
J. Am. Chem. Soc. 2015, 137, 3140−3156

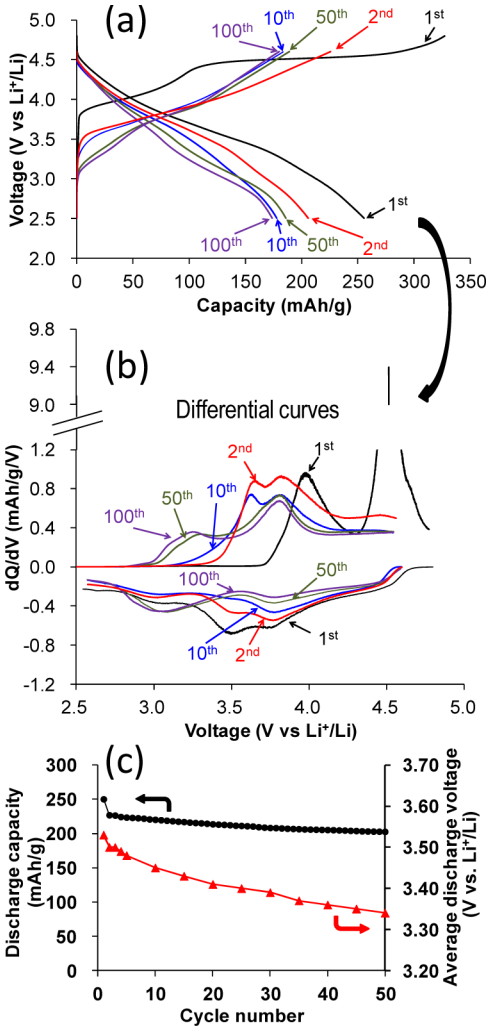

Figure 3. Comparison of charge and discharge curves obtained for Li//$Li_{1.20}Ni_{0.13}Mn_{0.54}Co_{0.13}O_2$ cells for different cycle numbers (a) and the corresponding differential curves $dQ/dV = f(V)$ (b). Changes in the discharge capacity and in the average discharge voltage versus the cycle number (c). Adapted from: Koga, H.; Croguennec, L.; Ménétrier, M.; Mannessiez, P.; Weill, F.; Delmas, C. Different oxygen redox participation for bulk and surface: A possible global explanation for the cycling mechanism of $Li_{1.20}Mn_{0.54}Co_{0.13}Ni_{0.13}O_2$. *J. Power Sources* **2013**, *236*, 250. Copyright (2013) Elsevier.

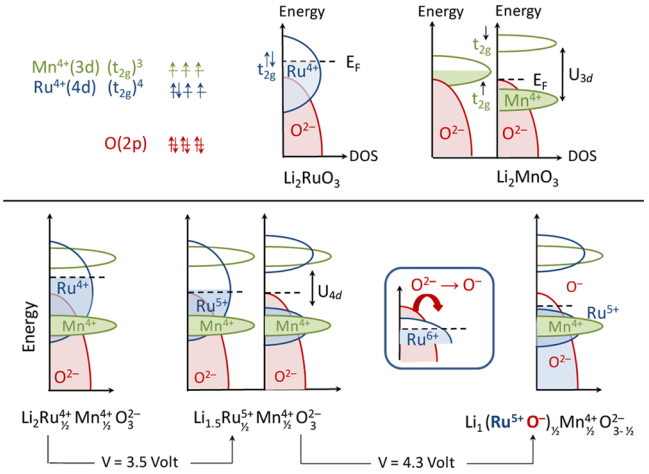

Figure 4. Schematic representations of the density of states (DOS) of Li_2RuO_3, Li_2MnO_3, and $Li_{2-x}Ru_{1/2}Mn_{1/2}O_3$ in which the Fermi level (E_F) line. This figure illustrates the more electronegative character of Ru compared to Mn, the stronger Ru(4d)-O(2p) hybridization compared to Mn(3d)-O(2p) and the electronic levels involved in the redox processes, i.e., the $Ru^{4+}(t_{2g})$ band from $x = 2$ to 1.5 and the O(2p) from $x = 1.5$ to 1.0. Reprinted with permission from:[42] Sathiya, M.; Ramesha, K.; Rousse, G.; Foix, D.; Gonbeau, D.; Prakash, A. S.; Doublet, M. L.; Hemalatha, K.; Tarascon, J.-M. *Chem. Mater.* **2013**, *25*, 1121. Copyright (2013) with American Chemical Society.

"dense" layered type or defective domains commonly denoted "splayered" (i.e., intermediate between layered and spinel)[44−47] (Figure 3). The kinetics of the surface modification and thus the fraction of "splayered" structure formed depend not only on the powder specific surface area[46] but also on the composition.[48] Indeed, the intrinsic stability of each transition metal M^{n+} in the intermediate tetrahedral sites in the pathways for diffusion/migration (Figure 2) governs the destabilization of oxidized oxygen ions and thus the degree of structural reorganization.

While it is clear that the largest advantage of Li-rich layered oxides lies in their outstanding capacities (>230 mAh/g), they suffer from a continuous voltage decay upon cycling which is the main handicap to their practical implementation (Figure 3).[49−51] It is induced by the irreversible structural modifications occurring at the outer part of the particles (that determine the potential measured). Using $Li_2Ru_{1-y}Sn_yO_3$ as a model compound, for which oxygen anions participate in the redox process with neither oxygen loss nor migration of transition metal ions, Sathiya et al. elegantly demonstrated that it is possible to tailor the composition of layered oxides to achieve high voltages with large reversible capacity and low fading with no voltage decay.[48] The proof of concept being demonstrated, the challenge is now to develop alternative compounds containing low cost and environmentally friendly metals as electronegative as possible to promote the participation of oxygen anions in the redox processes and hence larger reversible capacities. Thus, tailoring of the composition is an imperious track to follow to stabilize these Li-rich layered oxides for commercial viability. The transition metals of choice must be unstable in tetrahedral sites to avoid migration and thus prevent structural reorganization and voltage hysteresis. An alternative interesting approach to block or at least delay the structural reorganization is partial substitution by cations that do not participate to the redox processes and are stable in tetrahedral sites.[52]

Knowing that the redox processes in these compounds involve oxygen anions with the exchange of a larger number of electrons per transition metal, compositions with heavier transition metals such as 4d elements now become attractive. Therefore, a large panel of compositions can be designed with the formulas $Li_4MM'O_6$ (MM′ being $M^{II}M'^{VI}$, $M^{III}M'^{V}$, or $M^{IV}M'^{IV}$)[53] and Li_3MRuO_5 (MRu = $Co^{III}Ru^{IV}$ or $Ni^{II}Ru^{V}$ which could be expressed as $0.5Li_2RuO_3.0.5LiMO_2$ or as $Li[Li_xM_{1-3x}Ru_{2x}]O_2$ with $x = 0.2$) which are well worth exploring.[54]

The findings reported above clearly illustrate that in order to achieve attractive reversible capacities, the oxidation (charge) should proceed to high voltages (>4.6 V vs Li^+/Li, Figure 3), i.e., at the limit of the stability of the currently used electrolytes. Thus, interfacial chemistry offers an interesting research playground as surface properties have a direct impact on the irreversible capacity and rate capability. Approaches based on the formation of coated, core−shell or concentration gradient

DOI: 10.1021/ja507828x
J. Am. Chem. Soc. 2015, 137, 3140−3156

architectures have proved to be effective to modify the surface chemistry and thus its reactivity.[55−57] Well beyond the stabilization of the active material versus transition metal dissolution and electrolyte degradation, we think that the formation of these complex architectures could also promote stabilization of the surface versus oxygen loss and subsequent transition-metal rearrangement at the outer part of the particles.

In our opinion the road is still long and winding before the lithium-excess layered oxides may reach the application level. Nevertheless, the recent results indicate feasibility. Furthermore, the reversible participation of oxygen anions in the redox mechanism and the possibility of lithium-ion diffusion through a 3D channel of percolating vacancies, even in disordered structures, provide exciting perspectives for the development of new high capacity and high energy density insertion positive electrode materials.

2.2. 3D Structures. *2.2.1. Spinel Frameworks.* The 3D negative electrode materials so far studied are mainly based on the Ti^{4+}/Ti^{3+} redox couple[58] and exhibit insertion potentials between 1.5 and 2 V vs Li^+/Li. Such high potentials induce a severe penalty in the energy density as compared to carbonaceous anodes, but bring enhanced safety.[59] Indeed, at these potentials the electrolyte is stable, and no SEI formation is *a priori* expected. Furthermore, the risk of lithium metal deposition at high current (fast charging) is suppressed. From a more technological point-of-view, such materials enable the use of aluminum current collectors at the negative electrode (which would form alloys with lithium at low potential using graphite) replacing the heavy and expensive copper. The different TiO_2 polymorphs, also well investigated for a myriad of other applications, have received significant attention.[60,61] Yet, they do exhibit somewhat too high operation potentials for a negative electrode, and $Li_4Ti_5O_{12}$ is the only titanium-based compound having reached the commercial stage. It exhibits a defect spinel structure that can be described as $[Li]_{8a}[Li_{1/3}Ti_{5/3}]_{16d}[O_4]_{32e}$ and intercalates three lithium ions per formula unit (175 mAh/g) at 1.55 V vs Li^+/Li to form $Li_7Ti_5O_{12}$ with almost no changes in the lattice volume,[62] being thus termed "zero strain material". This fact has made possible the fundamental study of nanosize effects in absence of strains and interface energy, which is uncommon for electrode materials.[63] As $Li_4Ti_5O_{12}$ is electronically insulating, intense efforts have been devoted to increase its conductivity through doping or coating approaches, and hereby adequate performance at high charge/discharge rates (rate capability) has been widely reported. The insulating character of pristine $Li_4Ti_5O_{12}$ is thus by no means a bottleneck for application, especially since during the early stages of lithium intercalation and titanium reduction formation and rapid propagation of percolating electronically conductive pathways takes place.[64,65] The practical use of titanium oxides in general is currently being challenged by concerns raised about their presumed stability toward the electrolyte[66−68] based on observation of gas evolution,[69,70] which was attributed to catalytic effects. However, recent reports attribute such phenomena to water impurities in the electrolyte,[71] and thus the controversy is not yet solved.

$LiMn_2O_4$, also exhibiting spinel structure, is an attractive alternative to $LiCoO_2$,[72,73] owing to the low cost, wider abundance, and low toxicity of manganese. It delivers a reversible capacity of 110 mAh/g at a potential around 4 V vs Li^+/Li. Nevertheless, it was rapidly shown to suffer from severe capacity fading at high temperatures related to dissolution of manganese, as Mn^{2+} species formed through disproportionation ($2Mn^{3+} \rightarrow Mn^{2+} + Mn^{4+}$) or acid leaching of $Li_{1-x}Mn_2O_4$ by HF arising from reaction of water impurities with the electrolyte salt. Different routes have been considered to stabilize $LiMn_2O_4$: (i) partial cationic or anionic substitution (Ni, Al, F, ect.) or (ii) surface modifications through the formation of a coating or the use of additives in the electrolyte, with overall only limited success.[13]

Another spinel compound which has captured researchers' attention is $LiNi^{II}_{0.5}Mn^{IV}_{1.5}O_4$.[74,75] It exhibits a high operating voltage (4.7 V vs Li^+/Li), which challenges conventional electrolyte stability, involving the Ni^{2+}/Ni^{3+} and Ni^{3+}/Ni^{4+} couples with the exchange of 0.5 Li^+ per transition metal (i.e., a reversible capacity of 135 mAh/g). Depending on the synthesis conditions, $LiNi_{0.5}Mn_{1.5}O_4$ can crystallize in two space groups, $P4_332$ and $Fd3m$, the transition metal ions Ni and Mn being ordered in two octahedral sites for the former and randomly distributed for the latter. The disordered spinel is typically obtained at 900 °C, often with $Li_xNi_{1-x}O$ impurities, although Patoux et al. have shown that a disordered phase with composition $LiNi_{0.4}Mn_{1.6}O_4$ can be achieved pure.[76] The disordered phase exhibits lower capacity fading and higher rate capability, which has been related to its better electronic and ionic conductivities (Figure 5). Indeed, electrons delocalization occurs among manganese ($Mn^{3+}$and Mn^{4+}) and nickel (Ni^{2+}, Ni^{3+} and Ni^{4+}), whereas in the ordered phase $LiNi^{II}_{0.5}Mn^{IV}_{1.5}O_4$, the Ni^{2+} ions are isolated and surrounded by six non-active Mn^{4+} ions, preventing any mobility of the electrons. Mn dissolution is also less severe for the high voltage spinel $LiNi_xMn_{2-x}O_4$ than for $LiMn_2O_4$, as the content of Mn^{3+} ions in the spinel structure is minimized. Despite significant improvements, good performance in full cells needs to be fully confirmed, especially if involving storage at high potential and/or moderate temperature operation (Figure 5).

As in the case of some of the Li-rich materials discussed in the previous section one of the crucial issues for practical application is the absence of electrolytes compatible with operation at such high potentials. While results reported with electrolytes based in fluorinated carbonates and ethers, which oxidize at higher potentials and temperatures, are promising,[77−79] additives such as succinic and glutaric anhydrides have been proved to help in forming effective SL that behaves as polymer electrolyte[80] and thus may pave the way to success.

2.2.2. Polyanionic Frameworks. Since the demonstration by Padhi et al. that lithium ions can be extracted reversibly from olivine $LiFePO_4$ at ca. 3.5 V vs Li^+/Li (two-phase mechanism involving a Li-poor $Li_\varepsilon FePO_4$ phase and a Li-rich $Li_{1-\varepsilon'}FePO_4$ phase),[81] this positive electrode material has received considerable attention from the scientific community which has ultimately led to commercialization and is widely described in recent reviews.[63,82,83] One of the main breakthroughs in this path lies in the formation of a thin conductive carbon coating at the surface of $LiFePO_4$ nanoparticles[84] as a means to enhance electronic conductivity. After that seminal work, innumerable studies focused on different aspects and, through a pathway involving large controversies, finally brought in-depth understanding of the behavior of this coumpound upon cycling and of its redox mechanism: Particle size has strong effects in the electrochemical signature of $LiFePO_4$, which can be rationalized in terms of interface energy (mainly associated with the strains induced by volume changes in volume at the two-phase reaction front). Thus, smaller size involves a reduction of the two-phase domain during operation[85−88] and a slightly higher

DOI: 10.1021/ja507828x
J. Am. Chem. Soc. 2015, 137, 3140−3156

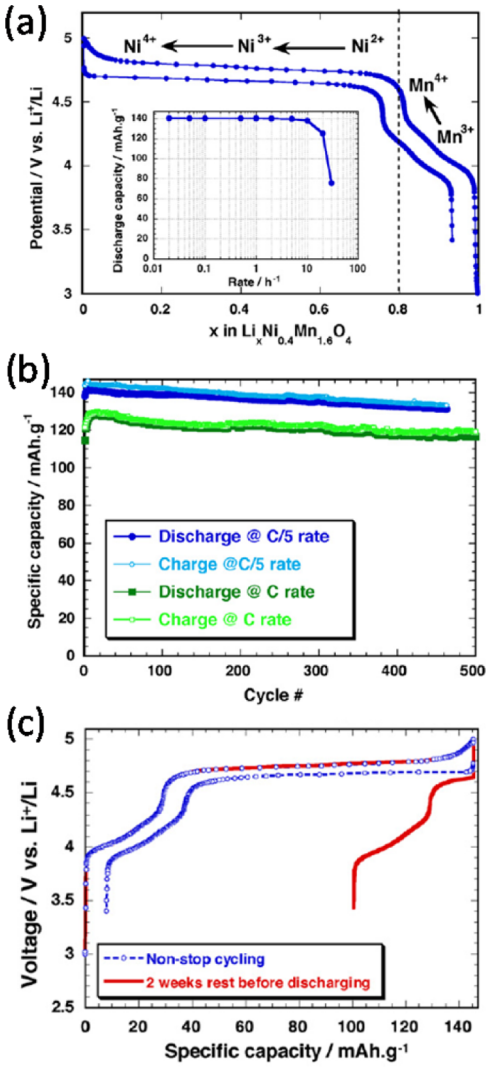

Figure 5. (a) Potential-composition profile of the non-stoichiometric and non-ordered $LiNi_{0.4}Mn_{1.6}O_4$ spinel oxide vs lithium at C/5 rate and at 20 °C: the specific capacity vs discharge rate is given in the inset. The small amount of Mn^{3+} ions is first oxidized to Mn^{4+}, and then Ni^{2+} ions are oxidized to Ni^{3+} and Ni^{4+}. (b) Specific capacity vs cycle number obtained at C and C/5 rates at 20 °C. (c) Illustration of the effect of a 2 weeks storage at high voltage, cycling was performed at C/5 at 20 °C. Adapted from:[76] High voltage spinel oxides for lithium-ion batteries: From the material research to the application. Patoux, S.; Daniel, L.; Bourbon, C.; Lignier, H.; Pagano, C.; Le Cras, F.; Jouanneau, S.; Martinet, S. *J. Power Sources* **2009**, *189*, 344. Copyright (2009) Elsevier.

operation potential.[89,90] In the extreme case of a sample consisting of a wide size distribution of nanoparticles, the potential profile is not anymore a flat plateau but a sloping curve, the latter not being the signature of a solid solution reaction, but rather of a series of different size particles enduring a two phase process.

Recent investigations have focused on the dependence of the redox mechanism on the cycling rate. Depending on how far from the equilibrium each particle is, the particle size distribution and electronic conductivity of the electrode, different kinetic pathways may exist.[91−94] The intermediate phase $Li_{\sim 0.6}FePO_4$ is formed, as predicted by Monte Carlo simulations,[95] at medium (C/5) or high rates (10C) depending on the particle size, but it evolves at open-circuit toward the thermodynamically stable mixture of Li-rich $Li_{1-\varepsilon}FePO_4$ and Li-poor $Li_{\varepsilon'}FePO_4$ end-members. A larger distribution of solid solution compositions Li_xFePO_4 was observed upon cycling of $LiFePO_4$ nanoparticles at even higher rates (for instance at 60C) (Figure 6). These recent results allow to rationalize the uncommon high rate capabilities of $LiFePO_4$ despite its redox mechanism consisting (at the equilibrium) of a two phase reaction between two end members showing very bad transport properties. The strains induced at the reaction front by cycling conditions out of the equilibrium promote the formation of solid solutions with small polarons Fe^{2+}/Fe^{3+}, higher elecronic conductivities, and thus the possibility for lihium to diffuse at high rates, as it was also recently demonstrated for the olivine Na_xFePO_4.[12,96,97]

The fundamental research performed over the last 10 years on $LiFePO_4$ is a nice example of how synergies between experimental and theoretical research can step by step pave the way for a better understanding of the material and its operation mechanisms. However, this would not have been possible without the development of *in situ* characterization tools,[98−101] enabling to probe the mechanims involved at all length scales (material, electrode, and battery), whatever the state of charge or discharge, the cycling rate, and the storage and aging conditions.

Olivine phases containing alternative transition metal ions such as $LiMnPO_4$, $LiCoPO_4$, and $LiNiPO_4$ have also been investigated. While the latter two exhibit too high operation potentials to be used with common electrolytes, $LiMnPO_4$ operates at ca. 4.1 V vs Li^+/Li and exhibits an attractive theoretical capacity (170 mAh/g). Yet, its practical development has been plagued with a myriad of difficulties (poor electronic/ionic transport properties, chemical instability in the charged state, etc.).[82] Despite the fact that a large diversity of synthetic strategies has been explored to yield smaller particles and composites,[82,102] the above-mentioned shortcomings are not overcome, and the electrochemical performance remains poor, especially at rates higher than C/5. Nevertheless, $LiMn_yFe_{1-y}PO_4$[103] for $y < 0.6$ has been found to exhibit a reversible capacity close to that of $LiFePO_4$ (for similar particle size) with higher average potential and very good rate capability.[104] As for $LiFePO_4$, solid solutions mechanisms would be at the origin of remarkable fast lithium diffusion in these Mn and Fe mixed compositions[104] as well as in vanadium-substituted $LiFePO_4$.[105]

Research on these alternative polyanionic materials has been boosted by the success of $LiFePO_4$ and the large panel of compositions and structures with different metal and different polyanions available to the solid-state chemist (see Figure 7).[82,106] The targets are achieving large energy densities by enhancing the operation potential, increasing the capacity through the number of electrons (lithium ions)[107] exchanged per transition metal ion considering two-electron couples as Ni^{2+}/Ni^{4+}, V^{3+}/V^{5+}, and Fe^{2+}/Fe^{4+}, and increasing the capacity through a decrease in the formula weight, considering for instance borates as an alternative to phosphates. Nevertheless, finding new polyanionic positive electrode materials with attractive properties remains challenging. Those that deserve, in our opinion, special attention are described below.

Sulfate chemistry has been intensively explored in the past few years, and as a result, many new materials with different structures and compositions have been synthesized:[108−112] the Tavorite, Silimanite, and Triplite $LiMSO_4F$, the layered $LiMSO_4OH$, and the Marinite $Li_2M(SO_4)_2$ (Figure 8). Iron-

DOI: 10.1021/ja507828x
J. Am. Chem. Soc. 2015, 137, 3140−3156

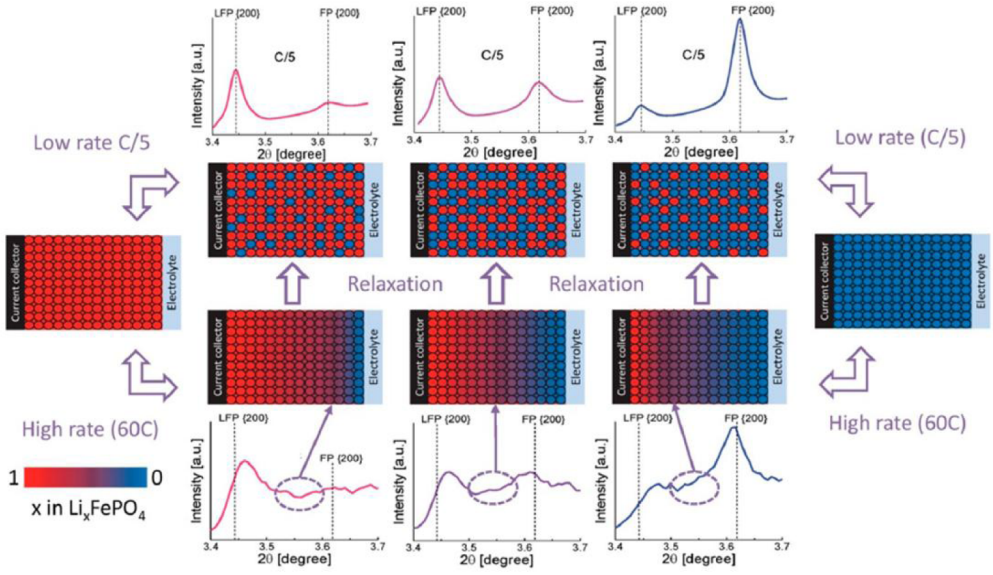

Figure 6. Model proposed by Zhang et al. to describe the phase distribution in $LiFePO_4$ electrodes at high and low rates or at open circuit. At low rates the electrode is near equilibrium, and no significant effect due to lithium concentration and polarization exists. As a consequence, the phase transition occurs randomly throughout the electrode, and only the two end member phases Li-poor $Li_\varepsilon FePO_4$ and Li-rich $Li_{1-\varepsilon'}FePO_4$ are observed. At high rates the polarization induces, depending on the particle size and electronic conductivity within the electrode, a potential gradient and a distribution of solid solution compositions within and between the particles. Reprinted with permission from:[93] Zhang, X.; van Hulzen, M.; Singh, D. P.; Brownrigg, A.; Wright, J. P.; van Dijk, N. H.; Wagemaker, M. *Nano Lett.*, **2014**, *14*, 2279. Copyright (2014) American Chemical Society.

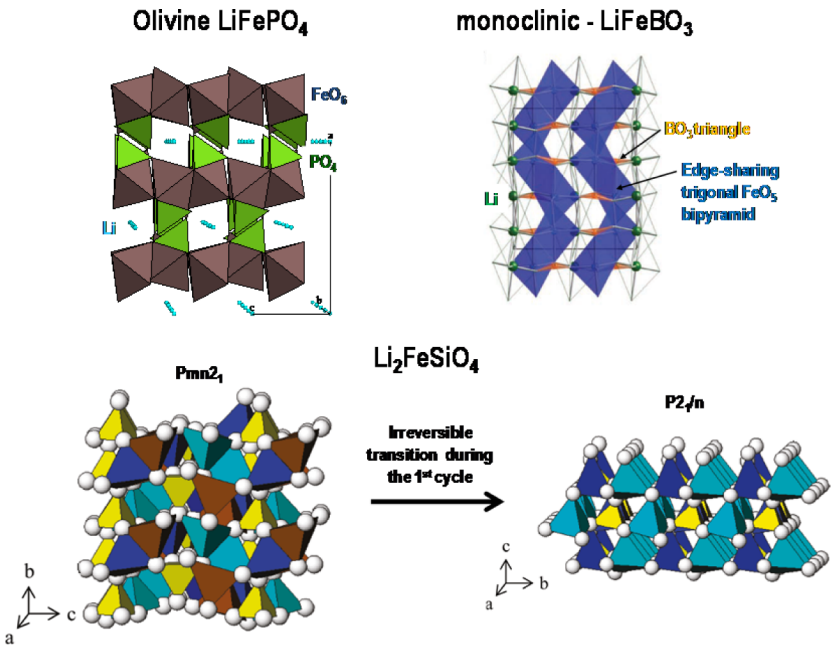

Figure 7. Description of different polyanionic structures: the olivine $LiFePO_4$, the monoclinic $LiFeBO_3$[118] (adapted from Yamada, A.; Iwane, N.; Harada, Y.; Nishimura, S.; Koyama, Y.; Tanaka, I. *Adv. Mater.*, **2010**, 22, 3583. Copyright (2010) WILEY-VCH Verlag GmbH & Co. KGaA, Weinheim) and Li_2FeSiO_4 as pristine and after the first cycle[119] (adapted with permission from Armstrong, A. R.; Kuganathan, N.; Islam, M. S.; Bruce, P.G. *J. Am. Chem. Soc.*, **2011**, 133, 13031. Copyright (2011) American Chemical Society).

based compounds are of peculiar interest as iron is an abundant element. They can exchange almost one electron per mol, especially when coated with a conducting polymer.[113] The clever use of the inductive effect, as nicely exemplified by J. B. Goodenough et al.[114,115] in Nasicon-type structure $Li_xM_2(XO_4)_3$ (M = V, Fe, Ti; X = P, W, S), has enabled to tailor the potential of the Fe^{2+}/Fe^{3+} redox couple in the Tavorite framework $LiFeXO_4Y$ (X = P, S; Y = OH, F) from 2.6 to 3.6 V vs Li^+/Li and then moving to the Triplite and Marinite polymorphs to values well above that observed for the olivine $LiFe^{II}PO_4$ (3.45 V). Triplite $LiFeSO_4F$ delivers the highest voltage at 3.9 V vs Li^+/Li, and understanding the driving force behind difference in potential between the two $LiFeSO_4F$ polymorphs[116] is crucial, as it can foster the development of other polyanionic families such as pyrophosphates.[117] The Triplite $LiFeSO_4F$ illustrates that materials with disordered structure (Li/Fe occupy the same octahedral site) can exhibit high energy density if organized enough to create a 3D

DOI: 10.1021/ja507828x
J. Am. Chem. Soc. 2015, 137, 3140−3156

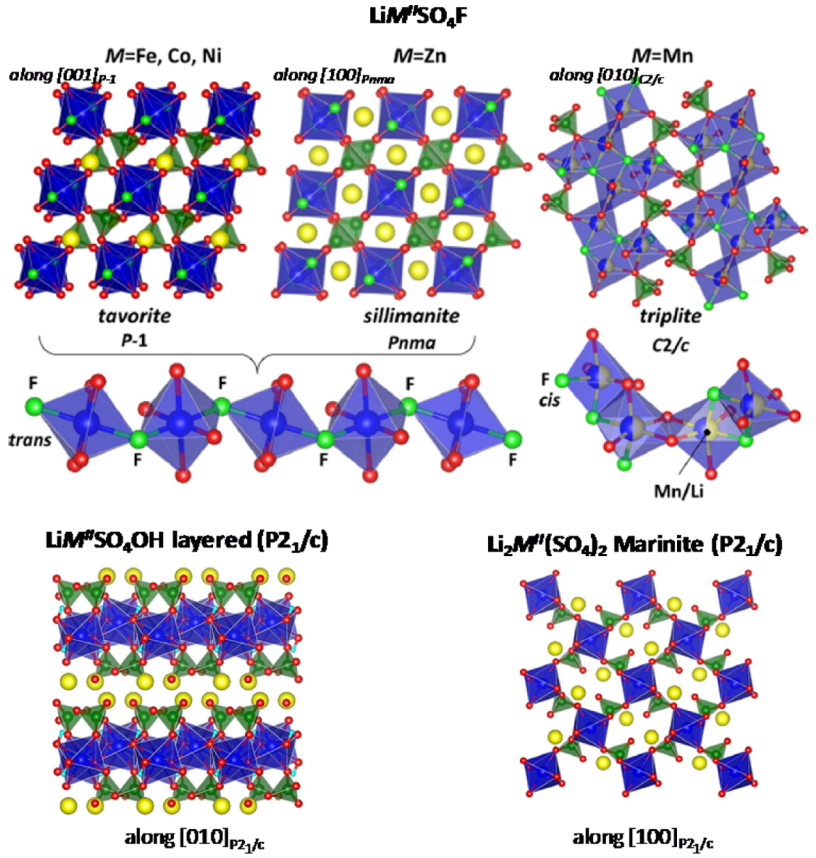

Figure 8. Comparison of the different structures obtained for $LiMSO_4F$, $LiMSO_4OH$, and $Li_2M(SO_4)_2$. MO_4F_2 and MO_6 octahedra are displayed in blue, SO_4 tetrahedra in green, and the Li^+ ions as yellow balls. Tavorite and Sillimanite are viewed perpendicular to the MO_4F_2 corner-sharing chains. For the Triplite, the MO_4F_2 octahedra are built of four oxygen and two fluorine atoms, and they are statistically filled with Li and M. For the layered hydroxysulfates, the layers are made of corner-sharing chains. For the Marinite, each MO_6 octahedron is isolated and surrounded by six sulfate groups. Adapted with permission from:[108] Rousse, G.; Tarascon, J. M. *Chem. Mater.* **2014**, *26*, 394. Copyright (2014) American Chemical Society.

diffusion pathway for fast lithium diffusion. From a "practical" application perspective, low cost synthesis, optimized morphologies, and composites have still to be developed to get the highest reversible capacity and cyclability for such compounds.

Phosphates showing Tavorite framework $LiMPO_4Y$ (M = Fe, Ti, Mn, V; Y = F, O, OH) are appealing as they exhibit a wide compositional spectrum.[82] The V-based compounds, $Li-V^{III}PO_4F$ and $LiV^{IV}PO_4O$, are attractive due to fast lithium diffusion at high voltage (>4.0 V vs Li^+/Li), and the possibility to exchange two electrons per metal (with the involvement of the redox couples V^{4+}/V^{3+} and V^{3+}/V^{2+} for the former and V^{5+}/V^{4+} and V^{4+}/V^{3+} for the latter). Nonetheless, the reversible capacity really achieved (140 mAh/g) corresponds to one electron per metal, as the difference between the two redox couples is >1.5 V, a value too large for practical consideration.[120−124] Even in such circumstances, $LiVPO_4F$ and $LiVPO_4O$ remain of interest as they deliver the highest energy density among all the polyanionic materials reported, with phosphates ensuring chemical and thermal stability. Silicates $Li_2M^{II}SiO_4$ (M = Fe, Mn, Ni) can also exhibit a wide range of polymorphs and compositions with Li, M, and Si occupying tetrahedral sites and Li and M being ordered or statistically distributed.[125−127] Again, the interest in these materials resides in the abundance of both Fe and Mn, and the possibility of exchanging two electrons per transition metal, which has unfortunately not been achieved to date. The current research focus is engineering of particle size, morphology, carbon coating, etc., in order to optimize the electronic wiring between the nanoparticles, the lithium diffusion within the particles, and thereby electrochemical performance.[128−130] Nonetheless, both the rate capability and reversible capacity (most often given for a wide potential window 1.5−4.8 V vs Li^+/Li) remain poor.[131]

Last but not least, borates are especially interesting due to their lower formula weight.[132] $LiM^{II}BO_3$ (M = Fe, Mn, Co) are investigated, and diverse strategies such as engineering of the active nanoparticles are attempted to reach high reversible capacity,[133−136] but success is very limited for $LiFeBO_3$ (130 mAh/g vs the theoretical 210 mAh/g at C/20 and 55 °C, within a large voltage window 2.0−4.5 V vs Li^+/Li)[137] and even worse for $LiMnBO_3$ and $LiCoBO_3$.[138,139] Interestingly, capacity values close to theoretical (201 $mAhg^{-1}$) at C/50 and room temperature have been reported for $LiMn_{0.5}Fe_{0.4}Mg_{0.1}BO_3$,[140] although the origin of this remarkable behavior (i.e., easier lithium diffusion for that peculiar composition) remains to be understood.

Overall, phosphates and sulfates remain the most attractive playground for the research of new positive electrode materials. Several compounds exhibiting rather fast lithium diffusion and thus good reversible capacity and cyclability have already been identified, even if optimization of the particle size and of the electrode formulation is often required to achieve decent performance. The main penalty of sulfates versus phosphates is their solubility, which prevents any electrode slurry preparation in water and causes accelerated aging upon storage. After years

DOI: 10.1021/ja507828x
J. Am. Chem. Soc. 2015, 137, 3140−3156

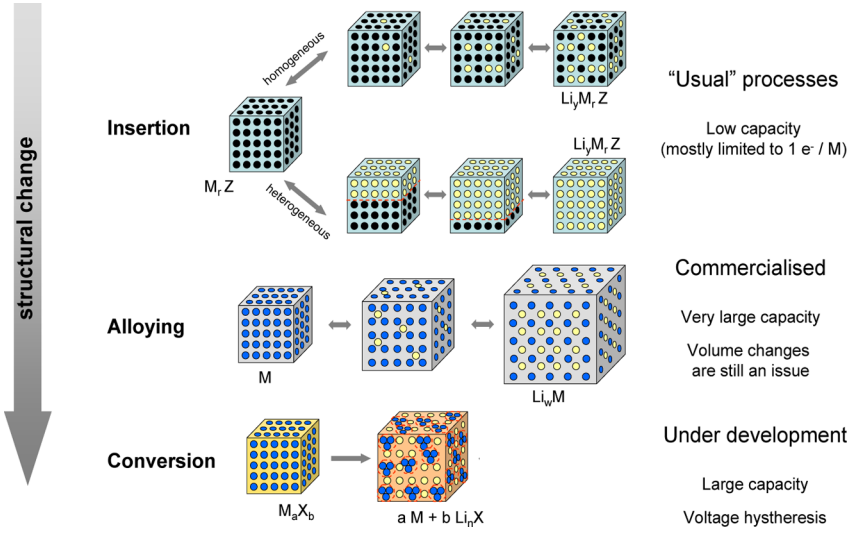

Figure 9. Schematic representation of different reaction mechanisms observed in electrode materials for lithium batteries. Black circles: voids in the crystal structure, blue circles: metal, yellow circles: lithium. Reproduced from:[152] Palacin, M. R. *Chem. Soc. Rev.* **2009**, *38*, 2565, with permission from The Royal Society of Chemistry.

of research devoted to borates and silicates, little progress has been achieved due to (i) the difficulty to control the synthesis (purity and nature of the polymorph) and (ii) the very bad transport properties associated with the presence of defects at the surface of the material or within the bulk and irreversible structural modifications observed upon cycling. Alternative syntheses are widely developed to design new materials and new structures, especially at low temperature using sometimes biology inspired processes.[141] As an example, a myriad of new sulfate polymorphs were for instance recently obtained using ionothermal methods.[142−144] On another ground theoretical studies have revealed to be a very powerful tool to predict defect chemistry (Li/M disorder, extra M in the cavities, etc.), surfaces' energy, lithium diffusion pathways, etc. to guide the solid-state chemist in tailoring the shape (size and growth according to preferential orientations) and the stoichiometry of the particles for optimized performances[145,146] while also bringing insights on the stable electronic and crystal structures. In contrast the identification of new materials from scratch by theoretical approaches[147] can still be challenged by intuition of the experienced chemist.[148]

3. ALTERNATIVE REACTION MECHANISMS

Materials that exhibit a non-insertion-based redox reaction mechanism with lithium are not new, as the electrochemical formation of alloys was already demonstrated in the 1970s,[149] and the first reports on partial reversibility for the mechanism currently termed "conversion reaction"[150] also trace back to the 1980's.[151] The main advantage of such alternative reaction pathways (see Figure 9) is the large increase in electrochemical capacity (i.e., moles of lithium/electrons reacted per mol of material), while the main drawback is that this is only achieved at the expense of major structural changes, which are obviously caused by the large modification in the composition of the material. As an example, the formation of $Li_{15}Si_4$ for Si electrodes results in an increase of 375% in the number of atoms present in each active particle with electrochemical capacities of 8363 mAh/cm^3 and 3589 mAh/g, much larger than the 975 mAh/cm^3 and 372 mAh/g achieved for graphite (formation of LiC_6 with 16% increase in the number of atoms per active particle). Unfortunately, these changes are difficult to "buffer", even with the use of sophisticated strategies and typically result in cycling performance penalties. While significant advances were made for alloys and some seem to be almost on the commercialization pipeline, the progress in overcoming the bottlenecks associated with conversion reactions is stagnating and prospects of practical application vanishing.

3.1. Alloys. Alloying reactions between lithium and a large number of metallic or semimetallic elements have proved feasible in electrochemical cells at room temperature in conventional organic electrolytes and have been widely studied.[153,154] Considerations of achievable capacities coupled to abundance, cost and toxicity restrict the systems deserving interest for application[155] to a handful of choices; Si, Sn, Al and Pb, with the first two clearly being the most attractive (3589 mAh/g to 8363 mAh/cm^3 and 991 mAh/g to 7233 mAh/cm^3 for Si and Sn, respectively) with Si having deserved most attention in recent years. The practical utilization of alloy electrodes is handicapped by the huge volume changes associated with the (de)alloying process, which result in the introduction of large strains in the particles that promote microcrack formation and propagation. Such changes lead upon cycling to a progressive decohesion, particle shuffling, and, subsequently, to severe capacity fading. A wide spectrum of materials engineering strategies has been developed[155] to limit the effects of these volume changes, based on different considerations such as the better accommodation of volume changes for particles that are amorphous, nanosized, and less prone to break upon stress, or porous,[156] since the available voids could be filled during the volume expansion. Along the same line, the use of active particles embedded in a conducting matrix (i.e., carbon) which could buffer the volume expansion has also been widely explored. Unfortunately these approaches do also involve drawbacks related to the use of nanosized materials such as lower tap densities and higher surface/volume ratios and promote enhanced reactivity with the electrolyte. Another successful alternative, although probably tricky to implement at the full cell level, is the limitation in the extent of reduction proposed for silicon in 2007.[157] Non-reacted silicon

DOI: 10.1021/ja507828x
J. Am. Chem. Soc. 2015, 137, 3140−3156

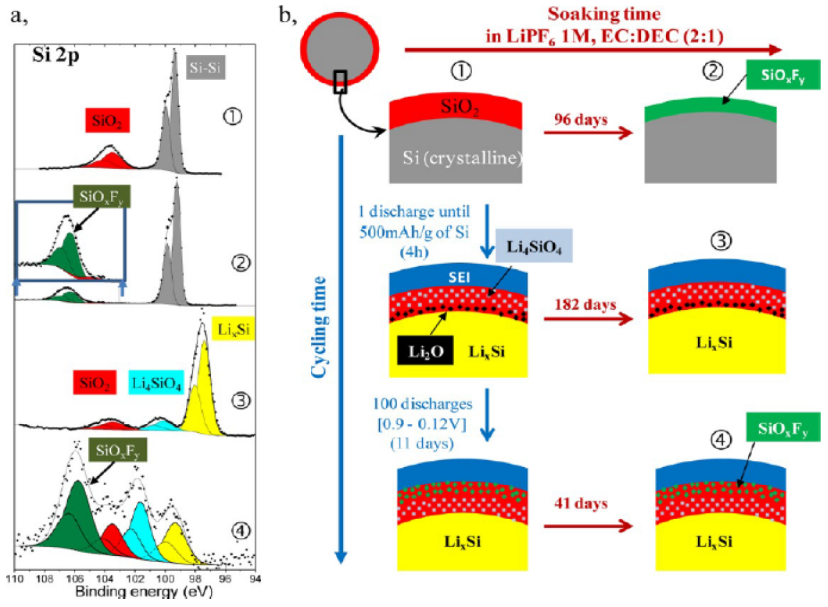

Figure 10. (a) Si 2p spectra (in-house PES, 1486.6 eV) of ① a silicon-based pristine electrode, ② an electrode after 96 days in contact with the electrolyte, ③ after a first reduction to provide 500 mAh/g_{Si} and ④ after the 100th reduction to 0.12 V. (b) Schematic view of the layer formed on the silicon particle surfaces during cycling and/on storage with the electrolyte. Reprinted with permission from:[165] Philippe, B.; Dedryvere, R.; Gorgoi, M.; Rensmo, H.; Gonbeau, D.; Edstrom, K. *Chem. Mater.* **2013**, *25*, 394. Copyright (2013) American Chemical Society.

at the core of particles remains crystallized and helps in limiting the loss of integrity for the outer shell, which reacts and turns and remains amorphous during the lithium uptake and removal. The fundamentals of this approach are essentially the same as the use of thin active material films on an inert substrate so that reduction induces an expansion which is constrained to the direction perpendicular to the film. In this case, and in line with the above-mentioned strategies, amorphous films are preferred to avoid any anisotropic expansion of oriented grains during alloying. Intermetallics (MM′) have also been studied where M′ (Mn, Fe, Co, Ni, Cu, Nb, etc.) does not alloy with lithium (and hence brings about a decrease in the overall capacity) but contributes to buffer volume changes. In this case, the reduction process entails a displacement reaction with "extrusion" of M′ concomitant to the formation of the Li_xM alloy.[158−160] Similarly, but involving two metal forming alloys, the pseudobinary Sn−Si−C system has been addressed through combinatorial sputtering methods,[161] as Sn−Si alloys are specially interesting by their improved electrical conductivity and phase stability and carbon inhibits Sn segregation.

All those strategies are linked to the use of substrates (dense films, limited reaction), voids (porous powders), matrix (composite materials), all inactive or kept unreacted and therefore leading to a penalty in energy density. Moreover, capacities reported for these composites in the literature have to be taken with care, as they are often specified with respect to the mass of active material and not of composite. Despite all such drawbacks, these strategies have enabled huge improvements in performance with respect to graphite at the laboratory scale, mostly in the so termed "half-cells" using lithium counter-electrodes. However, a proper assessment of the capacity retention in full cells against conventional positive electrodes is still a crucial issue[162] not trivial to solve. For the latter, electrode balancing (the ratio between positive and negative) can be an issue, as the lithium supply is limited by the positive electrode and thus the effect on capacity fading can be dramatic. While coating the material with lithium metal to compensate for first cycle low Coulombic efficiency (mostly related to the formation of the SEI and concomitant loss of lithium)[163] should help in alleviating such effects, up-scaling of the production would be by no means trivial. Overall, the progress needed to reach the market advances at slow pace, and only a few percents of Si is present in Si−C composites commercially used today.

The development of long cycle life electrodes is also correlated to the ability to engineer a stable SEI. While its composition mostly depends on the electrolyte used and thus, should not dramatically differ from the SEI observed for graphite negative electrodes,[2−4] minor changes can play important roles for long-term stability and capacity retention. Thorough non-destructive depth resolved XPS studies on SEI grown on silicon containing electrodes have enabled to point out the existence of interfacial phase transitions involving reactivity of the native SiO_2 layer with lithium to form a lithium silicate and a fluorinated SiO_xF_y phase arising from reactivity with HF impurities,[164,165] the microstructure/nature of the SEI depending on the history of the cycling (Figure 10).

All such findings need to be seriously taken into account as the role of the SEI layer is much more critical for alloying materials than for conventional insertion electrodes. Indeed, the SEI will break if its endurance limit is exceeded by the amplitude of the stresses generated at the electrode and fresh naked electrode surface will form on which an additional SEI would start to grow. If this is continuous, it would ultimately result in cell failure due to electrolyte consumption and loss of electrode porosity, with a decrease in its effective surface area and concomitant increase in its polarization.[166] Thus, SEI engineering strategies to promote SEI with enhanced stability and elasticity, involving for instance the use of additives, are crucial.[167−169]

Electrode engineering through formulation is also vital. While the chain polymeric network of PVDF (commonly used in graphite-based electrodes) inducing electrode elasticity was believed to help in preventing particle disconnection for alloy-

DOI: 10.1021/ja507828x
J. Am. Chem. Soc. 2015, 137, 3140−3156

based electrodes, the good performance of micron-size silicon particles[170] using a very brittle polymer such as carboxymethylcellulose (CMC) came as a surprise. These findings were rationalized through elucidation of the silicon-binder interactions,[171−173] as the bonds between the carboxyl groups of CMC and SiO_2 on the particle surface were proposed to reform if locally broken and hence exhibit a self-healing effect[174] (Figure 11). The promising results achieved with CMC prompted the study of other binders exhibiting carboxyl groups such as PAA (poly(acrylic acid)) or polysaccharides[175,176] and grants for further improvement through polymer design strategies.[177,178] On a related aspect, the reactivity of nanosized particles which may show catalytic activity toward the liquid medium used in electrode fabrication can also be an issue, which is also currently being addressed by tuning the SiO_2 surface layer.[179]

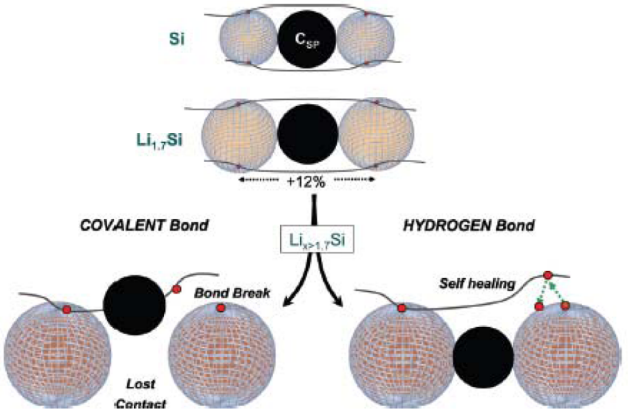

Figure 11. Schematic model showing the evolution in the CMC-Si bonding as lithium uptake proceeds, from top to bottom. Up to 1.7 Li/Si, both covalent and hydrogen bonding can sustain the particle volume changes, the overall swelling being buffered by the electrode porosity. Beyond 1.7 Si/Li, the maximum CMC stretching ability is reached and only the hydrogen-type Si-SMC interaction allows preservation of the efficient network through a self-healing process. Reproduced with permission from:[173] *J. Electrochem. Soc.*, **2011**, *158*, A750. Copyright 2011, The Electrochemical Society.

In summary, intense research efforts have resulted in important gains in performance and rational understanding of the reactivity of these complex systems, which holds promise for additional progress and gradual penetration of silicon-based electrodes in commercial cells.

3.2. Conversion Reactions. Conversion reaction is the term usually applied to define the reaction of a binary transition metal compound, M_aX_b (M = transition metal, X = O, S, N, P, F, H) with lithium to yield metallic nanoparticles embedded in a matrix of Li_yX according to $M_aX_b + (b{\cdot}n)\ Li \leftrightarrow a\ M + b\ Li_nX$, where n is the formal oxidation state of X. The typical potential vs composition profile of such materials is depicted in Figure 12. Depending on the starting compound some insertion of lithium in the pristine structure to form a ternary Li-M-X intermediate may take place at the beginning of reduction and this phase can further react through the conversion reaction itself, in other cases, if M does electrochemically form alloys with lithium, the conversion process may be followed by an alloying reaction. Independently of the complexity of the overall redox mechanism, the conversion step involving full reduction of the transition metal to its elemental state results in large capacity values, with for instance theoretical values of 700−1000 mAh/g for most oxides.[180] The key to the observed reversibility of the process upon subsequent oxidation seems to lie in the large amount of interfacial surface which makes nanoparticles very active toward the decomposition of the lithiated matrix. Even if simple at a first glance, such reactions induce a strong structural reorganization which, as in the case of alloys, may result in particle decohesion and unsatisfactory cycling performance.

The potential vs composition profile for conversion electrode materials does exhibit some characteristic features (see Figure 12), namely (i) low Coulombic efficiency (i.e., important irreversible capacity (IC)) on the first cycle, which exhibits a unique profile significantly different from the following ones; (ii) an additional extra capacity with respect to theoretical values (EC), its signature being a sloping curve that follows the conversion plateau; and (iii) large potential hysteresis (H) between oxidation and reduction (i.e., charge and discharge) which causes a large penalty in roundtrip energy efficiency and constitutes the major shortcoming to practical application for this kind of materials. The irreversible capacity has been

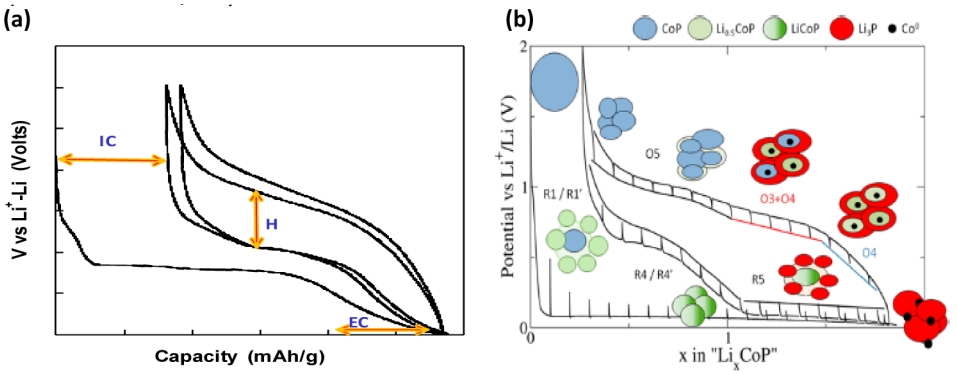

Figure 12. (a) Typical potential vs composition profile of the first two and half cycles for an electrode containing a material that reacts through a conversion reaction. The irreversible capacity (IC) upon the first cycle, extra capacity (EC) and potential hysteresis (H) are denoted by orange arrows. (b) GITT measurements carried out on a CoP/Li cell with steps of 1 h at C/10 (both upon oxidation and reduction) and rest to open circuit voltage until the potential slope is <30 mV/h. The experimental values are compared with theoretical predictions (colored lines for each step). (b) Reprinted with permission from:[196] Khatib, R.; Dalverny, A. L.; Saubanere, M.; Gaberscek, M.; Doublet, M. L. *J. Phys. Chem. C* **2013**, *117*, 837. Copyright (2013) American Chemical Society.

DOI: 10.1021/ja507828x
J. Am. Chem. Soc. 2015, 137, 3140−3156

ascribed to a limited reversibility of the reaction either due to the existence of electrically disconnected regions/particles within the electrode, as observed by *in situ* TEM[181] and/or to the reconversion to other phases than the initial compound (e.g the product of Co_3O_4 reduction forming CoO upon first reoxidation). As for the extra capacity (EC) phenomenon, two alternative explanations were initially proposed: interfacial charge storage[182,183] in a capacitive-like manner and electrolyte degradation,[184,185] with recent studies[186] indicating that interfacial storage would only account for a small percentage of the experimentally observed capacity, the rest being faradaic and fully related to electrolyte decomposition enhanced by the metal nanoparticles generated upon reduction. In the case of RuO_2 the process has been shown to be associated with the generation of LiOH and its subsequent reversible reaction with Li to form Li_2O and LiH.[187] Such parasitic side reaction would most probably end up in cell failure upon the long-term due to electrolyte consumption, but may be addressed by strategies involving active material particle coating, such as those discussed above for positive electrode materials operating at high potential, or by the use of alternative electrolytes.[188]

The origin of hysteresis (H) is still controversial. Electronic conductivity measurements carried out *in situ* in the course of reduction[189] rule out ohmic polarization as the main cause. This is also consistent with the fact that conversion electrodes can simultaneously show large voltage hysteresis and fast kinetics, i.e. when nanostructured current collectors are used[190] or with the fast conversion processes observed through real-time imaging.[191] Moreover, first-principles modeling on the Li-FeF_3 system revealed an inherent difference in reaction path between reduction and oxidation, determined by the limitations imposed by the need to transport a second species (e.g., Fe or F) in addition to Li.[192] Experimental studies using a large spectrum of techniques, including NMR, pair distribution function (PDF) analysis, and high-throughput electron microscopy techniques have allowed to confirm this trend not only for FeF_3 but also for FeO_xF_{2-x}.[193,194] DFT calculations on CoO and CoP considering the relative stability of the different interfaces that can be formed during the conversion process also point to an asymmetry of the chemical and electrical responses upon reduction and oxidation.[195,196] The computed data are in very good agreement with experimental results, the different potentials observed upon oxidation and reduction would be related to the growth of diverse interfaces which induce different electrochemical equilibria (see Figure 12). These findings have important implications, as strategies based on the reduction of diffusion lengths or the improvement of charge transfer kinetics, widely reported in the literature for materials operating through a conversion reaction mechanism, are clearly unlikely to produce any improvement in the hysteresis observed.

The operation potential of conversion reaction materials does obviously depend on both the transition metal and the anionic species, so that, in principle, a wide spectrum of choices would be available for different materials. Transition metal fluorides have the peculiarity to exhibit relatively high (>2 V vs Li^+/Li) potentials, as a result of the very high ionicity of the M-F bond, and hence are the only class of conversion reaction compounds suitable to be used as positive electrodes. They are, however, typically insulating and exhibit the largest potential hysteresis among all reported conversion reaction materials. Overall, oxides are by far the family of compounds that has attracted the most attention, with conversion reactions reported for a large diversity of phases[197] in the potential range 0.2−1.4 V vs Li^+/Li. The exception are those containing transition metals in groups 4 and 5, which would require much lower potentials to attain full reduction to metallic state.

Iron sulfides (both FeS_2 and FeS), which were studied in the 1980's in high temperature cells with molten salt electrolytes but abandoned due to their limited reversibilities, have recently been reinvestigated, together with nitrides, phosphides and even hydrides with only moderate success.[180] In the case of nitrides, phosphides, and certain sulfides, the redox centers are not exclusively located on the transition metal, but electron transfer occurs into bands that have a strong anion contribution, similarly to what has been mentioned above for some Li-rich layered positive electrode materials.[198] Hydrides have not deserved much attention and the few studies available reveal important capacity fading, but they remain the most interesting family to study from the fundamental point of view as they show the lowest hysteresis values reported.[199,200]

Overall, numerous studies on conversion reaction materials are available, largely focusing on improving cycle life and, to a lesser extent, on the Coulombic efficiencies. Partial success is achieved through electrode engineering strategies such as forming nanocomposites with nanosized active materials and a considerable amount of carbon. However, the practical relevance of thus results remains to be proven as particle reorganization and volume changes upon cycling are still likely to modify these nanostructures. Comparative studies of the performance of electrodes made of nano- and micron-sized particles offer diverging results, with the latter sometimes outperforming the former due to issues related to active material dissolution and catalytic activity toward electrolyte decomposition. It is unfortunate that a significant part of the publications dealing with conversion reaction materials do exclusively provide a plot of capacity vs cycle number to illustrate electrochemical performance, which does not allow to fully grasp the magnitude of the hysteresis. All in all, this is the main issue to tackle if such materials are ever to be seriously considered for any applications. Time will tell whether current research will result in a "natural selection" yielding some specific compounds (maybe hydrides even if they are currently not receiving any major attention) for which technological research can result in application prospects, as has been the case for silicon in alloys.

4. CONCLUSIONS AND PERSPECTIVES

Contrary to what *a priori* could be expected from the tremendous amount of research devoted to lithium-ion electrode materials and described in the previous sections, materials science development in the battery field is still crucial. Indeed, the energy density of cells will only significantly increase if the cell voltage and capacities of electrode materials are improved and the possibility of fast recharge can only be achieved through enabling redox reactions with fast kinetics. At the same time the extended cycle life must be maintained. Defining research strategies has to be made with due care in order to avoid following approaches proven unsuccessful in the past (the vast amount of literature available unfortunately largely contributes to overseeing previous meaningful work) and employ realistic targets. For instance, the compulsory presence of inert cell components makes the total increase in energy density of the cell with improving negative electrode capacities negligible after a certain threshold value[201] if the positive electrode capacities are not enhanced (Figure 13).

DOI: 10.1021/ja507828x
J. Am. Chem. Soc. 2015, 137, 3140−3156

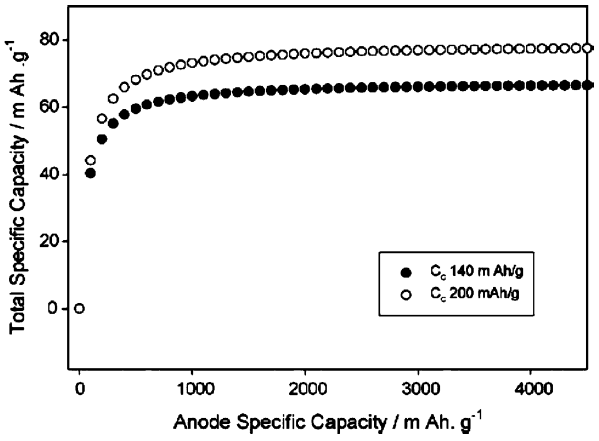

Figure 13. Total capacity of a 18650 lithium-ion cell as a function of the negative electrode (anode) capacity (C_A), (calculated taken into account the mass of inert cell components) for two different positive electrodes with capacities of 140 mAh/g (black filled circles) and 200 mAh/g (empty circles). Reprinted from:[201] Kasavajjula, U.; Wang, C.; Appleby, A. J. Nano- and bulk silicon-based insertion anodes for lithium-ion secondary cells. *J. Power Sources* **2007**, *163*, 1003. Copyright (2007), with permission from Elsevier.

Thus, if promises of commercialization for negative electrodes with a significant amount of silicon hold true, research efforts should target the positive counterpart. In view of the current state of the art, Li-rich layered oxides are most probably the most promising track to follow, with the reversible participation to the redox processes of oxygen anions and of 4d and 5d transition metal cations, the latter for some materials being able to exchange more than one electron per metal. A few alternatives would be Ru, Mo, or W though some of them are not viable from the practical point of view due to solubility, cost and/or abundancy constrains. The polyanionic materials exhibit higher thermal stability but are strongly penalized by a higher molecular weight. Success in the quest of the second electron per transition metal, if ever achieved, would undoubtedly bring these compounds to the front of the scene.

On the other hand, further attention to increased energy densities through the development of very high potential positive electrode materials must by all means be coupled to advances in electrolytes able to withstand such potentials without decomposing.

The advent of the lithium-ion battery technology and its continuously enhanced performance has been promoted by the development of inorganic electrode materials and the progresses in the basic understanding of their operating mechanisms at the atomic scale thanks to the ever improving characterization tools. Indeed, *in situ* or *operando* experiments are becoming routine or relatively common (X-ray or neutron diffraction[94,98−101] and also magnetic properties,[202] differential electrochemical mass spectroscopy (DEMS),[40] or Raman spectroscopy[203]) and efforts are carried out to adapt alternative characterization tools requiring specific environments (*in situ* TEM). The aim is to characterize electrodes probing all possible length scales from the atomic (NMR) to the electrode (tortuosity, tomography, magnetic resonance imaging),[204,205] including the SEI,[206] in order to ultimately enhance performance but also to understand aging processes[207] (much more complex to tackle) to enhance cycle life and thereby total energy throughput.

The basic research is evolving from the classical synthesis, characterization, and electrochemical testing approaches to embrace as well the technological aspects. Indeed, figures of merit for performance depend not only on the electrochemical testing parameters but also on the electrolyte, electrode formulation (type and amount of carbon and binder), and electrode architecture (thickness, porosity, active material loading etc.). Moreover, such studies more and more often involve moving from the model half-cells probing vs lithium counter-electrodes to the assembly of full cells, the latter forcing control of the SEI formation as well as careful electrode balancing, even at the laboratory scale.

The electrode slurry formulation has in the past largely been based on empirical observations and often kept as undisclosed industrial know-how. The topic has gradually captured also the interest of the academic community, why appealing correlations have been established between the type of polymer used as binder, the suspension rheological properties, the morphology (thickness, tortuosity, etc.)[208,209] and mechanical properties of the dried composite electrode, and the resulting electrochemical properties.[210−214] As current commercial cells do contain ca. 50% of inert components, a clear path to follow is the development of thick electrodes (>300 μm) with effective performance, which would also result in a cost decrease. This involves control of electrode architecture and porosity to ensure good kinetics for mass transport.

As a battery is an alive chemical reactor, gaining control of the performance through tuning materials properties require deep fundamental understanding of the processes taking place at all levels. There is no doubt that following such an integral approach will accelerate progress and help in selecting the most viable system for each application.

In conclusion, materials chemistry continues to be the essential part of battery research, and we are confident that with the currently available tools and focusing our efforts in the key current shortcomings, breakthroughs will certainly be unravelled in the years to come.

AUTHOR INFORMATION

Corresponding Author

*rosa.palacin@icmab.es

Notes

The authors declare no competing financial interest.

ACKNOWLEDGMENTS

We acknowledge ALISTORE-ERI and RS2E members for sharing fruitful discussions and Prof. Patrik Johansson, Prof. Dominique Larcher, and Dr Michel Ménétrier for critical reading of the text. We are grateful to Ministerio de Ciencia e Innovación (Spain, grant MAT2011-24757), CNRS, and Région Aquitaine for financial support. L.C. is grateful to C. Delmas, M. Ménétrier, D. Carlier, F. Weill, and C. Masquelier for their cooperative researches and valuable comments on different oxides and polyanionic systems as electrode materials for Lithium-ion batteries.

REFERENCES

(1) Whittingham, M. S. *Prog. Solid State Chem.* **1978**, *12*, 41.
(2) Xu, K. *Chem. Rev.* **2004**, *104*, 4303.
(3) Aurbach, D. *J. Power Sources* **2000**, *89*, 206.
(4) Verma, P.; Maire, P.; Novak, P. *Electrochim. Acta* **2010**, *55*, 6332.
(5) Xu, K.; von Cresce, A. *J. Mater. Chem.* **2011**, *21*, 9849.
(6) Goodenough, J. B.; Park, K. S. *J. Am. Chem. Soc.* **2013**, *135*, 1167.

DOI: 10.1021/ja507828x
J. Am. Chem. Soc. 2015, 137, 3140−3156

(7) Van der Ven, A.; Bhattacharya, J.; Belak, A. A. *Acc. Chem. Res.* **2013**, *46*, 1216.
(8) Flandrois, D.; Simon, B. *Carbon* **1999**, *37*, 165.
(9) Aurbach, D.; Markovsky, B.; Weissman, I.; Levi, E.; Ein-Eli, Y. *Electrochim. Acta* **1999**, *45*, 67.
(10) Endo, M.; Kim, C.; Nishimura, K.; Fujino, J.; Miyashita, K. *Carbon* **2000**, *38*, 183.
(11) Zheng, T.; Sue, J.; Dahn, J. R. *Chem. Mater.* **1996**, *8*, 389.
(12) Fong, R.; von Sacken, u.; Dahn, J. R. *J. Electrochem. Soc.* **1990**, *137*, 2009.
(13) Lee, K. T.; Jeong, S.; Cho, J. *Acc. Chem. Res.* **2013**, *46*, 1161.
(14) Guilmard, M.; Croguennec, L.; Denux, D.; Delmas, C. *Chem. Mater.* **2003**, *15*, 4476.
(15) Delmas, C.; Croguennec, L. *MRS Bull.* **2002**, *27*, 608.
(16) Ohzuku, T.; Makimura, Y. *Chem. Lett.* **2001**, *7*, 642.
(17) Ohzuku, T.; Makimura, Y. *Chem. Lett.* **2001**, *8*, 744.
(18) Sun, Y.-K.; Chen, Z.; Noh, H.-J.; Lee, D.-J.; Jung, H.-G.; Ren, Y.; Wang, S.; Yoon, C. S.; Myung, S.-T.; Amine, K. *Nat. Mater.* **2012**, *11*, 941.
(19) Myung, S.-T.; Noh, H.-J.; Yoon, S.-J.; Lee, E.-J.; Sun, Y.-K. *J. Phys. Chem. Lett.* **2014**, *5*, 671.
(20) Thackeray, M. M.; Kang, S.-H.; Johnson, C. S.; Vaughey, J. T.; Benedek, R.; Hackney, S. A. *J. Mater. Chem.* **2007**, *17*, 3112.
(21) Zhou, F.; Zhao, X.; Van Bommel, A.; Xia, X.; Dahn, J. R. *J. Electrochem. Soc.* **2011**, *158*, A187.
(22) Croy, J. A.; Abouimrane, A.; Zhang, Z. *MRS Bull.* **2014**, *39*, 407.
(23) Thackeray, M. M.; Johnson, C. S.; Vaughey, J. T.; Li, N.; Hackney, S. A. *J. Mater. Chem.* **2005**, *15*, 2257.
(24) Thackeray, M. M.; Kang, S.-H.; Johnson, C. S.; Vaughey, J. T.; Hackney, S. A. *Electrochem. Commun.* **2006**, *8*, 1531.
(25) Yu, H.; Ishikawa, R.; So, Y.-G.; Shibata, N.; Kudo, T.; Zhou, H.; Ikuhara, Y. *Angew. Chem., Int. Ed.* **2013**, *52*, 5969.
(26) Lu, Z.; Chen, Z.; Dahn, J. R. *Chem. Mater.* **2003**, *15*, 3214−3220.
(27) Lei, C. H.; Bareno, J.; Wen, J. G.; Petrov, I.; Kang, S.-H.; Abraham, D. P. *J. Power Sources* **2008**, *178*, 422−433.
(28) Wen, J. G.; Bareno, J.; Lei, C. H.; Kang, S. H.; Balasubramanian, M.; Petrov, I.; Abraham, D. P. *Solid State Ionics* **2011**, *182*, 98.
(29) Jarvis, K. A.; Deng, Z.; Allard, L. F.; Manthiram, A.; Ferreira, P. J. *Chem. Mater.* **2011**, *23*, 3614.
(30) Bareno, J.; Balasubramanian, M.; Kang, S. H.; Wen, J. G.; Lei, C. H.; Pol, S. V.; Petrov, I.; Abraham, D. P. *Chem. Mater.* **2011**, *23*, 2039.
(31) Koga, H.; Croguennec, L.; Mannessiez, Ph.; Ménétrier, M.; Weill, F.; Bourgeois, L.; Duttine, M.; Suard, E.; Delmas, C. *J. Phys. Chem. C* **2012**, *116*, 13497.
(32) McCalla, E.; Rowe, A. W.; Shunmugasundaram, R.; Dahn, J. R. *Chem. Mater.* **2013**, *25*, 989.
(33) McCalla, E.; Rowe, A. W.; Brown, C. R.; Hacquebard, P.; Dahn, J. R. *J. Electrochem. Soc.* **2013**, *160*, A1134.
(34) McCalla, E.; Lowartz, C. M.; Brown, C. R.; Dahn, J. R. *Chem. Mater.* **2013**, *25*, 912.
(35) McCalla, E.; Li, J.; Rowe, A. W.; Dahn, J. R. *J. Electrochem. Soc.* **2014**, *161*, A606.
(36) Long, B. R.; Croy, J. R.; Dogan, F.; Suchomel, M. R.; Key, B.; Wen, J.; Miller, D. J.; Thackeray, M. M.; Balasubramanian, M. *Chem. Mater.* **2014**, *26*, 3565.
(37) Weill, F.; Tran, N.; Croguennec, L.; Delmas, C. *J. Power Sources* **2007**, *172*, 893.
(38) Lee, J.; Urban, A.; Li, X.; Su, D.; Hautier, G.; Ceder, C. *Science* **2014**, *343*, 519.
(39) Lu, Z.; Dahn, J. R. *Electrochem. Solid-State Lett.* **2001**, *4*, A191.
(40) Armstrong, A. R.; Holzapfel, M.; Novàk, P.; Johnson, C. S.; Kang, S.-H.; Thackeray, M. M.; Bruce, P. G. *J. Am. Chem. Soc.* **2006**, *128*, 8694.
(41) Koga, H.; Croguennec, L.; Ménétrier, M.; Douhil, K.; Belin, S.; Bourgeois, L.; Suard, E.; Weill, F.; Delmas, C. *J. Electrochem. Soc.* **2013**, *160*, A786.
(42) Sathiya, M.; Ramesha, K.; Rousse, G.; Foix, D.; Gonbeau, D.; Prakash, A. S.; Doublet, M. L.; Hemalatha, K.; Tarascon, J.-M. *Chem. Mater.* **2013**, *25*, 1121.
(43) Sathiya, M.; Rousse, G.; Ramesha, K.; Laisa, C. P.; Vezin, H.; Sougrati, M. L.; Doublet, M. L.; Foix, D.; Gonbeau, D.; Walker, W.; Prakash, A. S.; Ben Hassine, M.; Dupont, L.; Tarascon, J.- M. *Nat. Mater.* **2013**, *12*, 827.
(44) Boulineau, A.; Simonin, L.; Colin, J.- F.; Canevet, E.; Daniel, L.; Patoux, S. *Chem. Mater.* **2012**, *24*, 3558.
(45) Boulineau, A.; Simonin, L.; Colin, J. F.; Bourbon, C.; Patoux, S. *Nano Lett.* **2013**, *13*, 3857.
(46) Koga, H.; Croguennec, L.; Ménétrier, M.; Mannessiez, P.; Weill, F.; Delmas, C. *J. Power Sources* **2013**, *236*, 250.
(47) Genevois, C. ; Koga, H. ; Croguennec, L. ; Ménétrier, M. ; Delmas, C. ; Weill, F. *J. Phys. Chem. C*, DOI: 10.1021/jp509388j.
(48) Sathiya, M. ; Abakumov, A. M.; Foix, D. ; Rousse, G. ; Ramesha, K.; Saubanère, M.; Doublet, M. L.; Vezin, H. ; Laisa, C. P. ; Prakash, A. S. ; Gonbeau, D. ; van Tendeloo, G. ; Tarascon, J.-M. *Nat. Mater.*, DOI:10.1038/NMAT4137.
(49) Croy, J. A.; Gallagher, K. G.; Balasubramanian, M.; Chen, Z.; Ren, Y.; Kim, D.; Kang, S.-H.; Dees, D. W.; Thackeray, M. M. *J. Phys. Chem. C* **2013**, *117*, 6525.
(50) Gallagher, K. G.; Croy, J. R.; Balasubramanian, M.; Bettge, M.; Abraham, D. P.; Burell, A. K.; Thackeray, M. M. *Electrochem. Commun.* **2013**, *33*, 96−98.
(51) Croy, J. R.; Gallagher, K. G.; Balasubramanian, M.; Long, B. R.; Thackeray, M. M. *J. Electrochem. Soc.* **2014**, *161*, A318.
(52) Lee, E.; Koritala, R.; Miller, D. J.; Johnson, C. S. *J. Electrochem. Soc.* **2015**, *162*, A322.
(53) Tarascon, J. M.; Sathiya, M.; Ramesha, K.; Abakumov, A. M.; Rousse, G.; Gonbeau, D.; Doublet, M. L.; Prakash, A. S.; Van Tendeloo, G. Proceedings from the 17th International Meeting on Lithium Batteries, Como, Italy, June 10−14, 2014; Electrochemical Society: Pennington, NJ, 2014; Abstract MA2014-01-103.
(54) Laha, S.; Moran, E.; Saez-Puche, R.; Alario-Franco, M. A.; Dos santos-Garcia, A. J.; Gonzalo, E.; Kuhn, A.; Natarajan, S.; Gopalakrishnan, J.; Garcia-Alvarado, F. *J. Mater. Chem. A* **2013**, *1*, 10686.
(55) Liu, J.; Reeja-Jayan, B.; Manthiram, A. *J. Phys. Chem. C* **2010**, *114*, 9528.
(56) Bettge, M.; Li, Y.; Sankaran, B.; Dietz Rago, N.; Spila, T.; Haasch, R. T.; Petrov, I.; Abraham, D. P. *J. Power Sources* **2013**, *233*, 346.
(57) Pol, V. G.; Li, Y.; Dogan, F.; Secor, E.; Thacheray, M. M.; Abraham, D. P. *J. Power Sources* **2014**, *258*, 46.
(58) Yang, Z.; Choi, D.; Kerisit, S.; Rosso, K.; Wang, D.; Zhang, J.; Graff, G.; Liu, J. *J. Power Sources* **2009**, *192*, 588.
(59) Chen, Z.; Belharouak, I.; Sun, Y. K.; Amine, K. *Adv. Funct. Mater.* **2013**, *23*, 959.
(60) Froschl, T.; Hormann, U.; Kubiak, P.; Kucerova, G.; Pfanzelt, M.; Weiss, C.; Behm, R.; Husig, N.; Kaiser, U.; Lfester, K.; Wohlfahrt-Mehrens, M. *Chem. Soc. Rev.* **2012**, *41*, 5313.
(61) Reddy, M. V.; Rao, G. V. S.; Chowdari, B. V. R. *Chem. Rev.* **2013**, *113*, 5364.
(62) Ohzuku, T.; Ueda, A.; Yamamoto, N. *J. Electrochem. Soc.* **1995**, *142*, 1431.
(63) Wagemaker, M.; Mulder, F. M. *Acc. Chem. Res.* **2013**, *46*, 1206.
(64) Song, M.; Benayad, A.; Choi, Y.; Park, K. *Chem. Commun.* **2012**, *48*, 516.
(65) Kim, C.; Norberg, N.; Alexer, C.; Kostecki, R.; Cabana, J. *Adv. Funct. Mater.* **2013**, *23*, 1214.
(66) Dominko, R.; Baudrin, E.; Umek, P.; Arcon, D.; Gaberscek, M.; Jamnik, J. *Electrochem. Commun.* **2006**, *8*, 673.
(67) Brutti, S.; Gentili, V.; Menard, H.; Scrosati, B.; Bruce, P. G. *Adv. Energy Mater.* **2012**, *2*, 322.
(68) Fehse, M.; Fischer, F.; Tessier, C.; Stievano, L.; Monconduit, L. *J. Power Sources* **2013**, *231*, 23.
(69) Belharouak, I.; Konig, G. M., Jr.; Tan, T.; Yumoto, H.; Ota, N.; Amine, K. *J. Electrochem. Soc.* **2012**, *159*, A1165.

DOI: 10.1021/ja507828x
J. Am. Chem. Soc. 2015, 137, 3140−3156

(70) He, Y. B.; Li, B.; Liu, M.; Zhang, C.; Lu, W.; Yang, C.; Li, J.; Du, H.; Zhang, B.; Yang, Q. Y.; Kim, J. K.; Kang, F. *Sci. Rep.* **2012**, *2*, 913.
(71) Bernhard, R.; Meini, S.; Gasteiger, H. A. *J. Electrochem. Soc.* **2014**, *161*, A497.
(72) Thackeray, M. M.; David, W. I. F.; Bruce, P. G.; Goodenough, J. B. *Mater. Res. Bull.* **1983**, *18*, 461.
(73) Amatucci, G.; Tarascon, J. M. *J. Electrochem. Soc.* **2002**, *149*, K31.
(74) Hu, M.; Pang, X.; Zhou, Z. *J. Power Sources* **2013**, *237*, 229.
(75) Manthiram, A.; Chemelewski, K.; Lee, E.-S. *Energy Environ. Sci.* **2014**, *7*, 1339.
(76) Patoux, S.; Daniel, L.; Bourbon, C.; Lignier, H.; Pagano, C.; Le Cras, F.; Jouanneau, S.; Martinet, S. *J. Power Sources* **2009**, *189*, 344.
(77) Zhang, Z.; Hu, L.; Wu, H.; Weng, W.; Koh, M.; Redfern, P.; Curtiss, L. A.; Amine, K. *Energy Environ. Sci.* **2013**, *6*, 1806.
(78) Hu, L.; Zhang, Z.; Amine, K. *Electrochem. Commun.* **2013**, *35*, 76.
(79) Markevich, E.; Salitra, G.; Fridman, K.; Sharabi, R.; Gershinsky, G.; Garsuch, A.; Semrau, G.; Schmidt, M. A.; Aurbach, D. *Langmuir* **2014**, *30*, 7414.
(80) Bouayad, H.; Wang, Z.; Dupré, N.; Dedryvére, R.; Foix, D.; Franger, S.; Martin, J.-F.; Boutafa, L.; Patoux, S.; Gonbeau, D.; Guyomard, D. *J. Phys. Chem. C* **2014**, *118*, 4634.
(81) Padhi, A. K.; Nanjundaswamy, K. S.; Goodenough, J. B. *J. Electrochem. Soc.* **1997**, *144*, 1188.
(82) Masquelier, C.; Croguennec, L. *Chem. Rev.* **2013**, *113*, 6552.
(83) Malik, R.; Abdellahi, A.; Ceder, G. *J. Electrochem. Soc.* **2013**, *160*, A3197.
(84) Ravet, N.; Chouinard, Y.; Magnan, J. F.; Besner, S.; Gauthier, M.; Armand, M. *J. Power Sources* **2001**, *97*−*98*, 503.
(85) Yamada, A.; Koizumi, H.; Nishimura, S. I.; Sonoyama, N.; Kanno, R.; Yonemura, M.; Nakamura, T.; Kobayashi, Y. *Nat. Mater.* **2006**, *5*, 357.
(86) Meethong, N.; Huang, H. Y. S.; Speakman, S. A.; Carter, W. C.; Chiang, Y. M. *Adv. Funct. Mater.* **2007**, *17*, 1115.
(87) Wagemaker, M.; Mulder, F. M.; van der Ven, A. *Adv. Mater.* **2009**, *21*, 1.
(88) Van der Ven, A.; Garikipati, K.; Kim, S.; Wagemaker, M. *J. Electrochem. Soc.* **2009**, *156*, A949.
(89) Van der Ven, A.; Wagemaker, M. *Electrochem. Commun.* **2009**, *11*, 881.
(90) Lee, K. T.; Kan, W. H.; Nazar, L. F. *J. Am. Chem. Soc.* **2009**, *131*, 6044.
(91) Orikasa, Y.; Maeda, T.; Koyama, Y.; Murayama, H.; Fukuda, K.; Tanida, H.; Arai, H.; Matsubara, E.; Uchimoto, Y.; Ogumi, Z. *J. Am. Chem. Soc.* **2013**, *135*, 5497.
(92) Sasaki, T.; Ukyo, Y.; Novák, P. *Nat. Mater.* **2013**, *12*, 569.
(93) Zhang, X.; van Hulzen, M.; Singh, D. P.; Brownrigg, A.; Wright, J. P.; van Dijk, N. H.; Wagemaker, M. *Nano Lett.* **2014**, *14*, 2279.
(94) Liu, H.; Strobridge, F. C.; Borkiewics, O. J.; Wiaderek, K. M.; Chapman, K. W.; Chupas, P. J.; Grey, C. P. *Science* **2014**, *344*, 1252817−1.
(95) Malik, R.; Zhou, F.; Ceder, G. *Natur. Mater.* **2011**, *10*, 587.
(96) Delacourt, C.; Poizot, P.; Tarascon, J. M.; Masquelier, C. *Nat. Mater.* **2005**, *4*, 254.
(97) Boucher, F.; Gaubicher, J.; Cuisinier, M.; Guyomard, D.; Moreau, P. *J. Am. Chem. Soc.* **2014**, *136*, 9144.
(98) Leriche, J. B.; Hamelet, S.; Shu, J.; Morcrette, M.; Masquelier, C.; Ouvrard, G.; Zerrouki, M.; Soudan, P.; Belin, S.; Elkaim, E.; Baudelet, F. *J. Electrochem. Soc.* **2010**, *157*, A606.
(99) Godbole, V. A.; Hess, M.; Villevieille, C.; Kaiser, H.; Colin, J. F.; Novak, P. *RSC Adv.* **2013**, *3*, 757.
(100) Bianchini, M.; Leriche, J. B.; Laborier, J.-L.; Gendrin, L.; Suard, E.; Croguennec, L.; Masquelier, C. *J. Electrochem. Soc.* **2013**, *160*, A2176.
(101) Roberts, M.; Biendicho, J. J.; Hull, S.; Beran, P.; Gustafsson, T.; Svensson, G.; Edstrom, K. *J. Power Sources* **2013**, *226*, 249.
(102) Ramar, V.; Saravanan, K.; Gajjela, S. R.; Hariharan, S.; Balaya, P. *Electrochim. Acta* **2013**, *105*, 496.
(103) Yamada, A.; Hosoya, M.; Chung, S.-C.; Kudo, Y.; Hinokuma, K.; Liu, K.-Y.; Nishi, Y. *J. Power Sources* **2003**, *119*−*121*, 232.
(104) Ravnsbæk, D. B.; Xiang, K.; Xing, W.; Borkiewicz, O. J.; Wiaderek, K. M.; Gionet, P.; Chapman, K. W.; Chupas, P. J.; Chiang, Y.-M. *Nano Lett.* **2014**, *14*, 1484.
(105) Omenya, F.; Chernova, N. A.; Zhang, R.; Fang, J.; Huang, Y.; Cohen, F.; Dobrzynski, N.; Senanayake, S.; Xu, W.; Whittingham, M. S. *Chem. Mater.* **2013**, *25*, 85.
(106) Rui, X.; Yan, Q.; Skyllas-Kazacos, M.; Lim, T. M. *J. Power Sources* **2014**, *258*, 19.
(107) Hautier, G.; Jain, A.; Mueller, T.; Moore, C.; Ong, S. O.; Ceder, G. *Chem. Mater.* **2013**, *25*, 2064.
(108) Rousse, G.; Tarascon, J. M. *Chem. Mater.* **2014**, *26*, 394.
(109) Tripathi, R.; Ramesh, T. N.; Ellis, B. L.; Nazar, L. F. *Angew. Chem., Int. Ed.* **2010**, *49*, 8738.
(110) Tripathi, R.; Popov, G.; Ellis, B. L.; Huq, A.; Nazar, L. F. *Energy Environ. Sci.* **2012**, *5*, 6238.
(111) Tripathi, R.; Popov, G.; Sun, X.; Ryan, D. H.; Nazar, L. F. *J. Mater. Chem. A* **2013**, *1*, 2990.
(112) Lander, L.; Reynaud, M.; Rousse, G.; Sougrati, M. T.; Laberty-Robert, C.; Messinger, R. J.; Deschamps, M.; Tarascon, J. M. *Chem. Mater.* **2014**, *26*, 4178.
(113) Sobkowiak, A.; Roberts, M. R.; Younesi, R.; Ericsson, T.; Häggström, L.; Tai, C.-W.; Andersson, A. M.; Edstrom, K.; Gustafsson, T.; Björefors, F. *Chem. Mater.* **2013**, *25*, 3020.
(114) Nanjundaswamy, K. S.; Padhi, A. K.; Goodenough, J. B.; Okada, S.; Ohtsuka, H.; Arai, H.; Yamaki, J. *Solid State Ionics* **1996**, *92*, 1.
(115) Padhi, A. K.; Nanjundaswamy, K. S.; Masquelier, C.; Goodenough, J. B. *J. Electrochem. Soc.* **1997**, *144*, 2581.
(116) Ben Yahia, M.; Lemoigno, F.; Rousse, G.; Boucher, F.; Tarascon, J. M.; Doublet, M. L. *Energy Environ. Sci.* **2012**, *5*, 9584.
(117) Ye, T.; Barpanda, P.; Nishimura, S.; Furuta, N.; Chung, S.-C.; Yamada, A. *Chem. Mater.* **2013**, *25*, 3623.
(118) Yamada, A.; Iwane, N.; Harada, Y.; Nishimura, S.; Koyama, Y.; Tanaka, I. *Adv. Mater.* **2010**, *22*, 3583.
(119) Armstrong, A. R.; Kuganathan, N.; Islam, M. S.; Bruce, P. G. *J. Am. Chem. Soc.* **2011**, *133*, 13031.
(120) Ateba Mba, J.-M.; Masquelier, C.; Suard, E.; Croguennec, L. *Chem. Mater.* **2012**, *24*, 1223.
(121) Bianchini, M.; Ateba-Mba, J. M.; Dagault, P.; Bogdan, E.; Carlier, D.; Suard, E.; Masquelier, C.; Croguennec, L. *J. Mater. Chem. A* **2014**, *26*, 10182.
(122) Harrison, K. L.; Bridges, C. A.; Segre, C. U.; Varnado, C. D.; Applestone, D.; Bielawski, C. W.; Paranthaman, M. P.; Manthiram, A. *Chem. Mater.* **2014**, *26*, 3849.
(123) Chen, Z.; Chen, Q.; Chen, L.; Zhang, R.; Zhou, H.; Chernova, N. A.; Whittingham, M. S. *J. Electrochem. Soc.* **2013**, *160*, A1777.
(124) Chen, Z.; Chen, Q.; Wang, H.; Zhang, R.; Zhou, H.; Chen, L.; Whittingham, M. S. *Electrochem. Commun.* **2014**, *46*, 67.
(125) West, A. R.; Glasser, F. P. *J. Solid State Chem.* **1972**, *4*, 20.
(126) Islam, M. S.; Dominko, R.; Masquelier, C.; Sirisopanaporn, C.; Armstrong, A. R.; Bruce, P. G. *J. Mater. Chem.* **2011**, *21*, 9811.
(127) Armstrong, A. R.; Sirisopanaporn, C.; Adamson, P.; Billaud, J.; Dominko, R.; Masquelier, C.; Bruce, P. G. *Z. Anorg. Allg. Chem.* **2014**, *640*, 1043.
(128) Peng, G.; Zhang, L. L.; Yang, X. L.; Duan, S.; Liang, G.; Huang, Y. H. *J. Alloys Compd.* **2013**, *570*, 1.
(129) Singh, S.; Mitra, S. *Electrochim. Acta* **2014**, *123*, 378.
(130) He, G.; Manthiram, A. *Adv. Funct. Mater.* **2014**, *33*, 5277.
(131) Gummow, R. J.; He, Y. *J. Power Sources* **2014**, *253*, 315.
(132) Legagneur, V.; An, Y.; Mosbah, A.; Portal, R.; Le Gal La Salle, A.; Verbaere, A.; Guyomard, D.; Piffard, Y. *Solid State Ionics* **2001**, *139*, 37.
(133) Yamada, A.; Iwane, N.; Harada, Y.; Nishimura, S.-i.; Koyama, Y.; Tanaka, I. *Adv. Mater.* **2010**, *22*, 3583.
(134) Yamashita, Y.; Barpanda, P.; Yamada, Y.; Yamada, A. *ECS Electrochem. Lett.* **2013**, *2*, A75.

DOI: 10.1021/ja507828x
J. Am. Chem. Soc. 2015, 137, 3140−3156

(135) Kim, J. C.; Moore, C.; Kang, B.; Hautier, G.; Jain, A.; Ceder, G. *J. Electrochem. Soc.* **2011**, *158*, A309.
(136) Yamada, A.; Iwane, N.; Nishimura, S. C.; Koyama, Y.; Tanaka, I. *J. Mater. Chem.* **2011**, *21*, 10690.
(137) Tao, L.; Rousse, G.; Chotard, J. N.; Dupont, L.; Bruyère, S.; Hanžel, D.; Mali, G.; Dominko, R.; Levasseur, S.; Masquelier, C. *J. Mater. Chem. A* **2014**, *2*, 2060.
(138) Li, S.; Xu, L.; Li, G.; Wang, M.; Zhai, Y. *J. Power Sources* **2013**, *236*, 54.
(139) Afyon, S.; Mensing, C.; Krumeich, F.; Nesper, R. *Solid State Ionics* **2014**, *256*, 103.
(140) Kim, J. C.; Seo, D. H.; Li, X.; Ceder G. https://ecs.confex.com/ecs/226/webprogram/Paper38372.html.
(141) Larcher, D.; Tarascon, J. M. *Nature* **2014**, *7*, 19.
(142) Recham, N.; Armand, M.; Laffont, L.; Tarascon, J.-M. *Electrochem. Solid-State Lett.* **2009**, *12*, A39.
(143) Recham, N.; Dupont, L.; Courty, M.; Djellab, K.; Larcher, D.; Armand, M.; Tarascon, J.-M. *Chem. Mater.* **2009**, *21*, 1096.
(144) Tarascon, J. M.; Recham, N.; Armand, M.; Chotard, J. N.; Barpanda, P.; Walker, W.; Dupont, L. *Chem. Mater.* **2010**, *22*, 724.
(145) Eames, C.; Clark, J. M.; Rousse, G.; Tarascon, J.-M.; Islam, S. *Chem. Mater.* **2014**, *26*, 3672.
(146) Clark, J. M.; Eames, C.; Reynaud, M.; Rousse, G.; Chotard, J. M.; Tarascon, J.-M.; Islam, M. S. *J. Mater. Chem. A* **2014**, *2*, 7446.
(147) Matts, I.; Chen, H.; Ceder, G. *ECS Electrochem. Lett.* **2013**, *2*, A81.
(148) Melot, B. C.; Tarascon, J. M. *Acc. Chem. Res.* **2013**, *46*, 1226.
(149) Dey, A. N. *J. Electrochem. Soc.* **1971**, *118*, 1547.
(150) Poizot, P.; Laruelle, S.; Grugeon, S.; Dupont, L.; Tarascon, J. M. *Nature* **2000**, *407*, 496.
(151) Godshall, N. A.; Raistrick, I. D.; Huggins, R. A. *Mater. Res. Bull.* **1980**, *15*, 561.
(152) Palacin, M. R. *Chem. Soc. Rev.* **2009**, *38*, 2565.
(153) Zhang, W. J. *J. Power Sources* **2011**, *196*, 13.
(154) Zhang, W. J. *J. Power Sources* **2011**, *196*, 877.
(155) Larcher, D.; Beattie, S.; Morcrette, M.; Edstrom, K.; Jumas, J. C.; Tarascon, J. M. *J. Mater. Chem.* **2007**, *17*, 3759.
(156) Cho, J. *J. Mater. Chem.* **2010**, *20*, 4009.
(157) Obrovac, M. N.; Krause, L. J. *J. Electrochem. Soc.* **2007**, *154*, A103.
(158) Yang, M. J.; Winter, M.; Besenhard, J. O. S. *Solid State Ionics* **1996**, *90*, 281.
(159) Yang, J.; Takeda, Y.; Imanishi, M.; Yamamoto, O. *J. Electrochem. Soc.* **1999**, *146*, 4009.
(160) Johnson, C. S.; Vaughey, J. T.; Thackeray, M.; Sarakonsri, T.; Hackney, S. A.; Fransson, L.; Edstrom, K.; Thomas, J. O. *Electrochem. Commun.* **2000**, *2*, 595.
(161) Al-Maghrabi, M. A.; Thorne, J. S.; Sanderson, R. J.; Byers, J. N.; Dahn, J. R.; Dunlap, R. A. *J. Electrochem. Soc.* **2012**, *159*, A711.
(162) Smith, A. J.; Burns, J. C.; Trussler, S.; Dahn, J. R. *J. Electrochem. Soc.* **2010**, *157*, A196.
(163) Liu, Bo.; Abouimrane, A.; Ren, Y.; Neuefeind, J.; Fang, Z. Z.; Amine, K. *J. Electrochem. Soc.* **2013**, *160*, A882.
(164) Philippe, B.; Dedryvere, R.; Allouche, J.; Lindgren, F.; Gorgoi, M.; Rensmo, H.; Gonbeau, D.; Edstrom, K. *Chem. Mater.* **2012**, *24*, 1107.
(165) Philippe, B.; Dedryvere, R.; Gorgoi, M.; Rensmo, H.; Gonbeau, D.; Edstrom, K. *Chem. Mater.* **2013**, *25*, 394.
(166) Oumellal, Y.; Delpuech, N.; Mazouzi, D.; Dupre, N.; Gaubicher, J.; Moreau, P.; Soudan, P.; Lestriez, B.; Guyomard, D. *J. Mater. Chem.* **2011**, *21*, 6201.
(167) Wachtler, M.; Besenhard, J. O.; Winter, M. *J. Power Sources* **2001**, *94*, 189.
(168) Ulldemolins, M.; Le Cras, F.; Pecquenard, B.; Phan, V. P.; Martin, L.; Martinez, H. *J. Power Sources* **2012**, *206*, 245.
(169) Wang, C.; Wu, H.; Chen, Z.; Mc Dowell, M. T.; Cui, Y.; Bao, Z. *Nat. Chem.* **2013**, *5*, 1042.
(170) Li, J.; Lewis, R. B.; Dahn, J. R. *Electrochem. Solid-State. Lett.* **2007**, *10*, A17.
(171) Lestriez, B.; Bahri, S.; Su, I.; Roue, L.; Guyomard, D. *Electrochem. Commun.* **2007**, *9*, 2801.
(172) Hochgatterer, N.; Schweiger, M.; Koller, S.; Rainmann, P.; Wohrle, T.; Wurm, C.; Winter, M. *Electrochem. Solid-State Lett.* **2008**, *11*, A76.
(173) Bridel, J. S.; Azais, T.; Morcrette, M.; Tarascon, J. M.; Larcher, D. *J. Electrochem. Soc.* **2011**, *158*, A750.
(174) Bridel, J. S.; Azais, T.; Morcrette, M.; Tarascon, J. M.; Larcher, D. *Chem. Mater.* **2010**, *22*, 1229.
(175) Kovalenko, I.; Zdyro, B.; Magasinski, A.; Hertzberg, B.; Milicev, Z.; Burtovy, R.; Yushin, G. *Science* **2011**, *334*, 75.
(176) Erk, C.; Brexesinski, T.; Sommer, H.; Schneider, R.; Janek, J. *ACS Appl. Mater. Interfaces* **2013**, *5*, 7299.
(177) Wu, M.; Xiao, X.; Vukmirovic, N.; Xun, S.; Prodip, K. D.; Song, X.; Olalde-Velasco, P.; Wang, D.; Weber, A. Z.; Wang, L. W.; Battaglia, V. S.; Yang, W.; Liu, G. *J. Am. Chem. Soc.* **2013**, *135*, 12048.
(178) Wang, C.; Wu, H.; Chen, Z.; Mc Dowell, M.; Cui, Y.; Bao, Z. *Nat. Chem.* **2013**, *5*, 1042.
(179) Touidjine, A.; Morcrette, M.; Courty, M.; Davoisne, C.; Lejeune, M.; Mariage, N.; Porchez, W.; Larcher, D. *(In preparation).*
(180) Cabana, J.; Monconduit, L.; Larcher, D.; Palacín, M. R. *Adv. Mater.* **2010**, *22*, E170.
(181) Gregorczyk, K. E.; Liu, Y.; Sullivan, J. P.; Rubloff, G. W. *ACS Nano* **2013**, *7*, 6354.
(182) Balaya, P.; Li, H.; Kienle, L.; Maier, J. *Adv. Funct. Mater.* **2003**, *13*, 621.
(183) Zhukovskii, Y. F.; Kotomin, E. A.; Balaya, P.; Maier, J. *Solid State Sci.* **2008**, *10*, 491.
(184) Laruelle, S.; Grugeon, S.; Poizot, P.; Dolle, M.; Dupont, L.; Tarascon, J. M. *J. Electrochem. Soc.* **2002**, *149*, A627.
(185) Gachot, G.; Grugeon, S.; Armand, M.; Pilard, S.; Guenot, P.; Tarascon, J. M.; Laruelle, S. *J. Power Sources* **2008**, *178*, 409.
(186) Ponrouch, A.; Taberna, P. L.; Simon, P.; Palacin, M. R. *Electrochim. Acta* **2012**, *61*, 13.
(187) Hu, Y. Y.; Liu, Z.; Nam, K. W.; Borkiewicz, O. J.; Cheng, J.; Hua, X.; Dunstan, M. T.; Yu, X.; Wiaderek, K. M.; Du, L. S.; Chapman, K. W.; Chupas, P. J.; Yang, X. Q.; Grey, C. P. *Nat. Mater.* **2013**, *12*, 1130.
(188) Gmitter, A. J.; Halajko, A.; Sideris, P. J.; Greenbaum, S. G.; Amatucci, G. G. *Electrochim. Acta* **2013**, *88*, 735.
(189) Sauvage, F.; Tarascon, J. M.; Baudrin, E. *J. Phys. Chem. C* **2007**, *111*, 9624.
(190) Taberna, P. L.; Mitra, S.; Poizot, P.; Simon, P.; Tarascon, J. M. *Nat. Mater.* **2006**, *5*, 567.
(191) Wang, F.; Yu, H. C.; Chen, M. H.; Wu, L.; Pereira, N.; Thornton, K.; Van der Ven, A.; Zhu, Y.; Amatucci, G. G.; Graetz, J. *Nature Comm.* **2012**, *3*, 1201.
(192) Doe, R. E.; Persson, K. A.; Meng, Y. S.; Ceder, G. *Chem. Mater.* **2008**, *20*, 5274.
(193) Yamakawa, N.; Jiang, M.; Key, B.; Grey, C. P. *J. Am. Chem. Soc.* **2009**, *131*, 10525.
(194) Sina, M.; Nam, K. W.; Su, D.; Pereira, N.; Yang, X. Q.; Amatucci, G. G.; Cosandey, F. *J. Mater. Chem. A* **2013**, *1*, 11629.
(195) Dalverny, A. L.; Filhol, J. S.; Doublet, M. L. *J. Mater. Chem.* **2011**, *21*, 10134.
(196) Khatib, R.; Dalverny, A. L.; Saubanere, M.; Gaberscek, M.; Doublet, M. L. *J. Phys. Chem. C* **2013**, *117*, 837.
(197) Reddy, M. V.; Rao, G. V. S.; Chowdari, B. V. R. *Chem. Rev.* **2013**, *113*, 5364.
(198) Doublet, M. L.; Lemoigno, F.; Gillot, F.; Monconduit, L. *Chem. Mater.* **2002**, *14*, 4126.
(199) Oumellal, Y.; Rougier, A.; Nazri, G. A.; Tarascon, J. M.; Aymard, L. *Nat. Mater.* **2008**, *7*, 916.
(200) Brutti, S.; Mulas, G.; Piciollo, E.; Panero, S.; Reale, P. *J. Mater. Chem.* **2012**, *22*, 14531.
(201) Kasavajjula, U.; Wang, C.; Appleby, A. J. *J. Power Sources* **2007**, *163*, 1003.
(202) Gershinsky, G.; Bar, E.; Monconduit, L.; Zitoun, D. *Energy Environ. Sci.* **2014**, *7*, 2012.

DOI: 10.1021/ja507828x
J. Am. Chem. Soc. 2015, 137, 3140−3156

(203) Novak, P.; Panitz, J.-C.; Joho, F.; Lanz, M.; Imhof, R.; Coluccia, M. *J. Power Sources* **2000**, *90*, 52.
(204) Chandrashekar, S.; Trease, N. M.; Chang, H. J.; Du, L. S.; Grey, C. P.; Jerschow, A. *Nat. Mater.* **2012**, *11*, 311.
(205) Ebner, M.; Marone, F.; Stampanoni, M.; Wood, V. *Science* **2013**, *342*, 716.
(206) Novak, P.; Goers, D.; Hardwick, L.; Holzapfel, M.; Scheifele, W.; Ufhiel, J.; Wursig, A. *J. Power Sources* **2005**, *146*, 15.
(207) Dubarry, M.; Liaw, B. Y.; Chen, M. S.; Chyan, S. S.; Han, K. C.; Sie, W. T.; Wu, S. H. *J. Power Sources* **2011**, *196*, 3420.
(208) Garcia, R. E.; Chiang, Y. M. *J. Electrochem. Soc.* **2007**, *154*, A856.
(209) Ebner, M.; Chung, D. W.; Garcia, R. E.; Wood, W. *Adv. Energy Mater.* **2014**, *4*, 1301278.
(210) Ligneel, E.; Lestriez, B.; Hudhomme, A.; Guyomard, D. *J. European Ceramic Soc.* **2009**, *29*, 925.
(211) Lestriez, B. *C. R. Chim.* **2010**, *13*, 1341.
(212) Zheng, H.; Li, J.; Song, X.; Liu, G.; Battaglia, V. S. *Electrochim. Acta* **2012**, *71*, 258.
(213) Zheng, H.; Zhang, L.; Liu, G.; Song, S.; Battaglia, V. S. *J. Power Sources* **2012**, *217*, 530.
(214) Bae, C. J.; Erdonmez, C. K.; Halloran, J. W.; Chiang, Y. M. *Adv. Mater.* **2013**, *25*, 1254.

DOI: 10.1021/ja507828x
J. Am. Chem. Soc. 2015, 137, 3140−3156